Densest local sphere-packing diversity. II. Application to three dimensions

Adam B. Hopkins, Frank H. Stillinger, and Salvatore Torquato

Phys. Rev. E **83**, 011304 — Published 31 January 2011

DOI: 10.1103/PhysRevE.83.011304

Densest local packing diversity. II. Application to three dimensions

Adam B. Hopkins and Frank H. Stillinger

Department of Chemistry, Princeton University, Princeton, New Jersey 08544

Salvatore Torquato

Department of Chemistry, Department of Physics,

Princeton Center for Theoretical Science,

Princeton Institute for the Science and Technology of Materials,

Program in Applied and Computational Mathematics,

Princeton University, Princeton, New Jersey 08544

School of Natural Sciences, Institute for Advanced Study, Princeton, New Jersey 08544

Abstract

The densest local packings of N three-dimensional identical nonoverlapping spheres within a radius $R_{min}(N)$ of a fixed central sphere of the same size are obtained for selected values of N up to $N = 1054$. In the predecessor to this paper [A.B. Hopkins, F.H. Stillinger and S. Torquato, Phys. Rev. E **81**, 041305 (2010)], we described our method for finding the putative densest packings of N spheres in d-dimensional Euclidean space $\mathbb{R}^d$ and presented those packings in $\mathbb{R}^2$ for values of N up to $N = 348$. We analyze the properties and characteristics of the densest local packings in $\mathbb{R}^3$ and employ knowledge of the $R_{min}(N)$, using methods applicable in any d, to construct both a realizability condition for pair correlation functions of sphere packings and an upper bound on the *maximal* density of *infinite* sphere packings. In $\mathbb{R}^3$, we find wide variability in the densest local packings, including a multitude of packing symmetries such as perfect tetrahedral and imperfect icosahedral symmetry. We compare the densest local packings of N spheres near a central sphere to minimal-energy configurations of $N + 1$ points interacting with short-range repulsive and long-range attractive pair potentials, e.g., $12-6$ Lennard-Jones, and find that they are in general completely different, a result that has possible implications for nucleation theory. We also compare the densest local packings to finite subsets of stacking variants of the densest infinite packings in $\mathbb{R}^3$ (the Barlow packings) and find that the densest local packings are almost always most similar, as measured by a *similarity metric*, to the subsets of Barlow packings with the smallest number of coordination shells measured about a single central sphere, e.g., a subset of the FCC Barlow packing. Additionally, we observe that the densest local packings are dominated by the dense arrangement of spheres with centers at distance $R_{min}(N)$. In particular, we find two "maracas" packings at $N = 77$ and $N = 93$, each consisting of a few unjammed spheres free to rattle within a "husk" composed of the maximal number of spheres that can be packed with centers at respective $R_{min}(N)$.

PACS numbers: 61.46.Bc, 61.43.-j, 68.08.De, 82.60.Nh

I. INTRODUCTION

A packing is defined as a set of nonoverlapping objects arranged in a space of given dimension d. One packing problem in d-dimensional Euclidean space $\mathbb{R}^d$ that has not been generally addressed is that of finding the maximally dense (optimal) packing(s) of N nonoverlapping d-dimensional spheres of unit diameter near (local to) an additional fixed central sphere such that the greatest radius R from any of the surrounding spheres' centers to the center of the fixed sphere is minimized. This problem is called the densest local packing (DLP) problem [1], and the minimized greatest radius associated with number of spheres N is denoted by $R_{min}(N)$. In various limits, the DLP problem encompasses both the kissing number and (infinite) sphere packing problems [2]. The former is a special case of the DLP problem in that the kissing number K_d, or number of identical d-dimensional nonoverlapping spheres that can simultaneously be in contact with (kiss) a central sphere, is equal to the greatest N for which $R_{min}(N) = 1$, and the latter is equivalent to the DLP problem in the limit that $N \to \infty$.

The DLP problem for 13 spheres in $\mathbb{R}^3$ dates back to a debate between Newton and Gregory in 1694. Newton believed that only 12 identical spheres could simultaneously contact a central same-size sphere, while Gregory believed the correct number to be 13. The first rigorous proof that Newton was right came in 1953 [3], followed by a more concise proof in 1956 [4]. However, the question remains: how close can 13 identical spheres come to a central same-size sphere - how good was Gregory's guess? In another paper [1], we showed that for any d, the DLP optimal packings in $\mathbb{R}^d$ with $R_{min}(N) \leq \tau$, $\tau = (1+\sqrt{5})/2 \approx 1.618$ the golden ratio, include packings where all N sphere centers lie on a spherical surface of radius $R_{min}(N)$. The smallest radius spherical surface onto which the centers of 13 spheres of unit diameter can be placed is strongly conjectured to be $R = R_{min}(13) = 1.045573\ldots$, with the centers arranged in a structure first documented in [5]. It appears that though Gregory was incorrect in conjecturing K_3 to be 13, his guess wasn't particularly far-off.

For each N in the DLP problem in $\mathbb{R}^d$, there is a single optimal $R_{min}(N)$, though generally for a given N there can be multiple distinct packings that achieve this radius. In the predecessor to this paper [6], hereafter referred to as paper I, we studied the optimal packings and corresponding $R_{min}(N)$ for the DLP problem in $\mathbb{R}^2$ for $N = 1$ to $N = 109$ and for N corresponding to full shells of the triangular lattice from $N = 120$ to $N = 348$. We also

discussed the general concepts and applications associated with DLP optimal packings for arbitrary N and d.

In paper I, we reported that a majority of the DLP optimal packings in $\mathbb{R}^2$ contain rattlers, or spheres (disks) that can be displaced in at least one direction without increasing $R_{min}(N)$ or displacing any other sphere (disk) in the packing (i.e., a rattler is a sphere (disk) that is not locally jammed [34, 35]). Further, we found that many optimal packings contain cavities at their centers in which the central disk, were it not fixed, could move freely (as a rattler, or object in a packing that can be displaced without displacing any other objects or the packing boundary). The optimal packings in $\mathbb{R}^2$ also exhibit a wide range of rotational symmetries, particularly for smaller N, and packings of N spheres from certain classes such as the curved [7] and wedge hexagonal packings were found to be optimal at various N. We additionally observed that as N grows large, disks in the *bulk* (as opposed to on the surface) of DLP optimal packings are largely arranged as subsets of the densest infinite packing in $\mathbb{R}^2$, i.e., with centers on the sites of the triangular lattice, whereas disks farthest from the central sphere (centers at distance $R_{min}(N)$) tend to form circular rings.

The DLP problem is related to problems of finding arrangements of $N+1$ points $\mathbf{r}^{N+1} \equiv \mathbf{r}_1, \mathbf{r}_2, \ldots, \mathbf{r}_{N+1}$ that minimize potential energy. Defining the DLP potential energy as the negative of the density of $N+1$ spheres (including the central sphere) contained completely within the *encompassing sphere*, a sphere of radius $R+1/2$ centered on the central sphere, the DLP problem becomes a minimal-energy problem with the pair potential between points (sphere centers) exhibiting features of long-range attraction and infinite short-range repulsion. Comparisons between DLP optimal packings and minimal-energy configurations for $N+1$ points with pair potentials exhibiting similar features of long-range attraction and short-range repulsion indicate that, though minimal energies for certain values of N are similar, optimal configurations of points (sphere centers) are in general completely different. This finding could have implications for nucleation theory, as is discussed in more detail in Secs. IV and VI.

The DLP problem is relevant to the realizability of functions that are candidates to be the pair correlation function of a packing of identical spheres. For a statistically homogeneous and isotropic packing, the pair correlation function is denoted by $g_2(r)$; it is proportional to the probability density of finding a separation r between any two sphere centers and normalized such that it takes the value of unity when no spatial correlations between cen-

ters are present. Specifically, no function can be the pair correlation function of a point process (where a packing of spheres of unit diameter is a point process with a minimum pair separation distance of unity) unless it meets certain necessary, but generally not sufficient, conditions known as realizability conditions [8–10]. Two of these conditions that appear to be particularly strong for the realizability of sphere packings [11] are the nonnegativity of $g_2(r)$ and its corresponding structure factor $S(k)$, where

$$S(k) = 1 + \rho\tilde{h}(k) \tag{1}$$

with number density ρ and $\tilde{h}(k)$ the d-dimensional Fourier transform of the total correlation function $h(k) \equiv g_2(r) - 1$.

Knowledge of the maximal number of sphere centers that may fit within radius R from an additional fixed sphere's center, where that maximal number, denoted by $Z_{max}(R)$, is equal to the greatest N in the DLP problem for which $R_{min}(N) \leq R$, may be employed to construct a third realizability condition, called the Z_{max} condition [1, 12, 13, 15], on $g_2(r)$. This condition is written

$$Z(R) \leq Z_{max}(R), \tag{2}$$

where $Z(R)$ is defined for a statistically homogeneous packing as the expected number of sphere centers within distance R from an arbitrary sphere center. The function $Z(R)$ can be related to the pair correlation function $g_2(r)$, where for a packing of spheres with a pair correlation function $g_2(\mathbf{r})$ that is direction-dependent, $g_2(r)$ is the directional average of $g_2(\mathbf{r})$, by

$$Z(R) = \rho s_1(1) \int_0^R x^{d-1} g_2(x) dx. \tag{3}$$

In Eq. (3), ρ is the constant number density of sphere centers and $s_1(r)$ is the surface area of a sphere of radius r in $\mathbb{R}^d$,

$$s_1(r) = \frac{2\pi^{d/2} r^{d-1}}{\Gamma(d/2)}. \tag{4}$$

As was discussed in previous papers [1, 12], the Z_{max} realizability condition has been shown to encode information not included in the nonnegativity conditions on pair correlation functions and their corresponding structure factors alone.

The maximal infinite-volume packing fraction ϕ_*^∞ of identical nonoverlapping spheres in $\mathbb{R}^d$ can be bounded from above by employing knowledge of the optimal $R_{min}(N)$ in the DLP

problem, where a *packing fraction* is the fraction of a given space covered by nonoverlapping objects. As was discussed in paper I, an upper bound is constructed by measuring the packing fraction $\phi(R+1/2)$ as the fraction of the volume of the encompassing sphere covered by the $N+1$ spheres of unit diameter,

$$\phi(R+1/2) = \frac{N+1}{(2R+1)^d} = \rho \frac{\pi^{d/2}}{2^d \Gamma(1+d/2)}. \tag{5}$$

In the first equality in (5), R is the greatest radius from any of the N surrounding spheres' centers to the center of the central sphere, and in the second equality, the number density ρ is the fraction of a sphere of radius $\phi(R+1/2)$ covered by the $N+1$ spheres of unit diameter and $\Gamma(x)$ is the standard gamma function.

For small numbers of spheres ($N \leq 1200$) in low dimensions ($d \leq 10$), an algorithm combining a nonlinear programming method with a stochastic search of configuration space can be employed on a personal computer to find putative solutions to the DLP problem. The accuracy of the solutions found by such an algorithm is bounded only by a machine's precision, and in general higher accuracy only requires more computation time. Using such an algorithm, the details of which are described in paper I, we find and present putatively-optimal DLP packings and their corresponding $R_{min}(N)$ in $\mathbb{R}^3$ for $N = 1$ to $N = 161$ (accuracy of at least 10^{-8} sphere diameters), and for selected values of N from $N = 176$ to $N = 1054$ (accuracy of at least 10^{-6} sphere diameters). Images and coordinates for many of the optimal packings that we have found are located on our website [16]. Of the $N \geq 176$ studied, some are randomly chosen and some correspond to the numbers of contacting spheres of unit diameter near and equal to the number in subsets of face-centered-cubic (FCC) and hexagonal-close-packed (HCP) packings with a given number of full coordination shells.

In $\mathbb{R}^3$ as in $\mathbb{R}^2$, rigorous and repeated testing of the algorithm indicates that it is robust in finding DLP optimal packings. The identification of rotation and reflection symmetry, spatially precise to 10^{-8} or better sphere diameters, in numerous DLP presumed-optimal packings in $\mathbb{R}^3$ for $N \leq 114$ supports this conclusion, as does our finding that the minimal R found for $N = 56$ to $N = 58$ and for $N \geq 60$ are smaller than the (previously) best-known minimal radii [17] for the less-restrictive problem of finding the minimal radius (larger) sphere into which $N+1$ spheres of unit diameter may be packed. However, the algorithm is

dependent upon initial conditions, and as the number N of spheres increases, an increasing number of trials have been necessary before we have found a packing and corresponding $R_{min}(N)$ that with a high degree of confidence we consider optimal. For this reason, due to computing time constraints, though we strongly conjecture that the vast majority of our packings are optimal for $N \leq 161$, as many as 50% or more of packings for $N \geq 176$ may not be strictly optimal (though we hereafter refer to them as optimal). For these packings, we will present evidence indicating that the smallest radius R found for each $N > 161$ is very near to the optimal $R_{min}(N)$, if not equal to it.

Over the range of N studied, DLP optimal packings in $\mathbb{R}^3$ differ substantially in terms of symmetry, contact networks, and spatial positioning from the Barlow packings [18], which we recall are the maximally dense infinite packings of identical nonoverlapping spheres in $\mathbb{R}^3$. In general, we find that optimal packings are dominated by the dense arrangement of spheres on their surface, i.e., those spheres with centers at precisely distance $R_{min}(N)$, where the arrangement of the spheres in the bulk (interior) is of secondary importance. Similarly in $\mathbb{R}^2$, DLP optimal packings differ substantially from packings of contacting disks arranged on the points of a triangular lattice, though in both dimensions at sufficiently large N, the spheres in the bulk of each optimal packing begin to always resemble, respectively, a subset of a corresponding maximally dense infinite packing in $\mathbb{R}^2$ or $\mathbb{R}^3$.

In $\mathbb{R}^2$, the approximate N and corresponding $R_{min}(N)$ at which this change occurs may be identified visually by perusing the DLP optimal packings at various N. In $\mathbb{R}^3$ however, it can be difficult to visually compare distinct packings. Consequently, we here introduce the concept of a *similarity metric*, defined as a metric designed to quantify the degree of similarity between one set of points and a reference set. As will be discussed in Sec. III, using such a metric allows quantitative comparisons of the relative degree of similarity between the radial spatial positions of spheres configured as DLP optimal packings and of spheres configured as subsets of a maximally dense infinite packing.

Our key results and findings are summarized in the following list:

- A novel realizability condition on candidate pair correlation functions $g_2(r)$ for sphere packings in $\mathbb{R}^3$ is constructed from knowledge of the $R_{min}(N)$ (Sec. II).

- DLP optimal packings for almost every N exhibit the phenomenon of surface-maximization, i.e., the number of spheres *on the surface* (with centers at precisely

radius $R_{min}(N)$) is either the maximal or nearly the maximal number that can be placed without overlap with centers on a spherical surface of radius $R = R_{min}(N)$ (Sec. III A). For two N ($N = 77$ and $N = 93$), the DLP optimal packings are termed "maracas" packings, as packings at these N have the maximal number of spheres on the surface, while all spheres *not* on the surface are rattlers (Sec. V E).

- DLP optimal packings for the N studied are almost always *most* similar to subsets of FCC Barlow packings, and for sufficiently large N, the bulk (as opposed to the surface) of optimal packings appear to always be structured similarly to a subset of a Barlow packing (Sec. III B).

- The set of N for which there are DLP optimal packings that include rattlers is unbounded, and the number of rattlers in a packing appears to grow *at most* as quickly as the surface area of the packing (Sec. III B).

- The 12−6 Lennard-Jones (LJ) energy of DLP optimal packings for some N are within a few percent of the minimal LJ energy for $N + 1$ points, but in general the spatial configurations of sphere centers in DLP optimal packings are completely different from the minimal-energy configurations of $N + 1$ points (Sec. IV).

- Many DLP optimal packings for $N \leq 114$ exhibit elements of perfect rotational and/or reflection symmetry (Secs. V B and V C).

- Imperfect icosahedral symmetry is present in many DLP optimal packings, but perfect icosahedral symmetry is *never* present (Sec. V D).

II. REALIZABILITY AND BOUNDS

A function that is a candidate to be the pair correlation function $g_2(r)$ of a point process, where a packing of spheres of unit diameter is a point process in which the minimum pair distance is unity, must be nonnegative for all r and correspondingly have a structure factor $S(k)$ that is nonnegative for all k. For a packing of spheres of unit diameter, such a candidate function must additionally be identically zero on the interval $[0, 1)$ to reflect the nonoverlap condition between spheres. However, the two nonnegativity conditions and the nonoverlap condition are only necessary, and generally not sufficient, conditions for a function to be

the pair correlation function of a sphere packing. The Z_{max} realizability condition further constrains candidate pair correlation functions, eliminating a range of functions that obey the two aforementioned nonnegativity conditions and are identically zero on $[0, 1)$, and yet violate the Z_{max} condition [1, 12].

The function $Z_{max}(R)$ in $\mathbb{R}^3$ can be compared to $Z_{Bar}(R)$, where $Z_{Bar}(R)$ is the largest number of spheres of unit diameter whose centers can be placed within distance R from a central sphere center when packings are constrained to the space of Barlow packings. Both $Z_{max}(R)$ and $Z_{Bar}(R)$ increase roughly linearly with R^3, as the volume of a sphere of radius R is proportional to R^3. The function $Z_{max}(R)$ is clearly always greater than or equal to $Z_{Bar}(R)$, but we find strict inequality, i.e., $Z_{max}(R) > Z_{Bar}(R)$, for $N \geq 13$, as can be seen in Figure 1, a plot of $Z_{max}(R)$ and $Z_{Bar}(R)$ vs. N for $N = 1$ to $N = 161$.

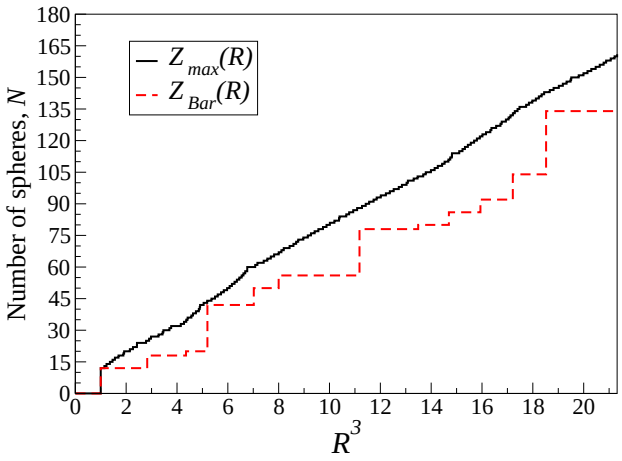

FIG. 1: (Color online) $Z_{max}(R)$ vs R^3, as determined by optimal and putatively optimal solutions to the DLP problem for $N = 1$ to $N = 161$, and $Z_{Bar}(R)$. The radius R of the disk enclosing the centers of the N identical (smaller) disks and same-size fixed disk is measured in units of the diameter of the enclosed disks.

We also compare each $R_{min}(N)$ that we have found to each minimal radius $R_{Bar}(N)$, where $R_{Bar}(N)$ is defined as the smallest R for N spheres surrounding a fixed central sphere when packings are constrained to the space of Barlow packings. Figure 2 plots $R_{min}(N)$ and $R_{Bar}(N)$ vs. N for $N = 1$ to $N = 161$ and for the values of N for which we used the algorithm to seek optimal packings from $N = 176$ to $N = 533$. It is clear from the figure that $R_{min}(N)$ rises roughly with $R_{Bar}(N)$, and that $R_{Bar}(N)$ is an upper bound for $R_{min}(N)$.

It is also true that $R_{Bar}(N)$ cannot grow too much larger than $R_{min}(N)$; Appendix A

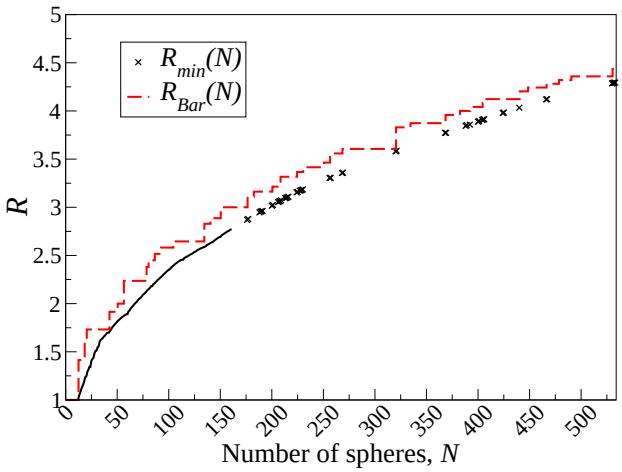

FIG. 2: (Color online) A plot of $R_{min}(N)$ vs. N for $N = 1$ to $N = 161$ and for selected values of $N \geq 176$ and $R_{Bar}(N)$ vs. N for $N = 1$ to $N = 533$.

discusses methods of bounding $R_{min}(N)$ in $\mathbb{R}^3$ from below using the Barlow packings. We do not here explicitly construct a lower bound for $R_{min}(N)$ that, along with the upper bound in Fig. 2, could be used to specify a range of feasible values for each optimal $R_{min}(N)$. However, we can comment on the accuracy of the presumed-optimal $R_{min}(N)$ found by the algorithm for $N \geq 176$ by comparing the differences between $R_{Bar}(N)$ and the putative $R_{min}(N)$ for $N \geq 176$ and over the range $N \leq 161$ for which we have confidence in the optimality of the packings. This comparison of $R_{Bar}(N) - R_{min}(N)$ over the two ranges yields values for both the smallest and largest differences that are very near to one another, as can be visually verified by close inspection of Fig. 2.

In $\mathbb{R}^3$, knowledge of the Barlow packings allows us to bound $R_{min}(N)$ and consequently $Z_{max}(R)$. However, in $\mathbb{R}^d$ with $d > 3$ where the maximal infinite-volume packing fraction ϕ_*^∞ is only known with analytical rigor for $d = 8$ and $d = 24$ [19], optimal $R_{min}(N)$ can be employed to provide a rigorous upper bound on ϕ_*^∞. As was shown in paper I, ϕ_*^∞ in $\mathbb{R}^d$ can be bounded from above with knowledge of any $R_{min}(N_*)$, where $N_* \in \mathbb{N}$ is the set of all positive integers for which N_* is the greatest integer N such that $R_{min}(N) = R_{min}(N_*)$. For example, in $\mathbb{R}^3$, $R_{min}(1) = ... = R_{min}(12) = 1$, where $N_* = 12$ is the greatest N for which $R_{min}(N) = 1$ [20].

The rigorous upper bound on ϕ_*^∞, proved in paper I, is

$$\phi_*^\infty \leq \hat{\phi}_*(N_*), \qquad N_* \in \mathbb{N}, \tag{6}$$

where the maximal local packing fraction $\hat{\phi}_*(N)$ of a packing of N nonoverlapping spheres of unit diameter around a same-size fixed central sphere is defined as the ratio of the volumes of the $N+1$ spheres to the volume of a sphere of radius $R_{min}(N)$, or

$$\hat{\phi}_*(N) = \frac{N+1}{(2R_{min}(N))^d}. \tag{7}$$

Though ϕ_*^∞ is known rigorously in $\mathbb{R}^3$ [14], it is informative to calculate the bounds derived from the putative $R_{min}(N_*)$ over the range of N tested. As N increases, the bound becomes sharper (becoming exact as $N \to \infty$), and calculations can give a sense of how quickly the bound approaches the known value of ϕ_*^∞. Figure 3 plots the upper bound calculated using relations (6) and (7) for the putative $R_{min}(N_*)$ found in $\mathbb{R}^3$ versus the proved maximal infinite-volume packing fraction, $\phi_*^\infty = \pi/\sqrt{18}$.

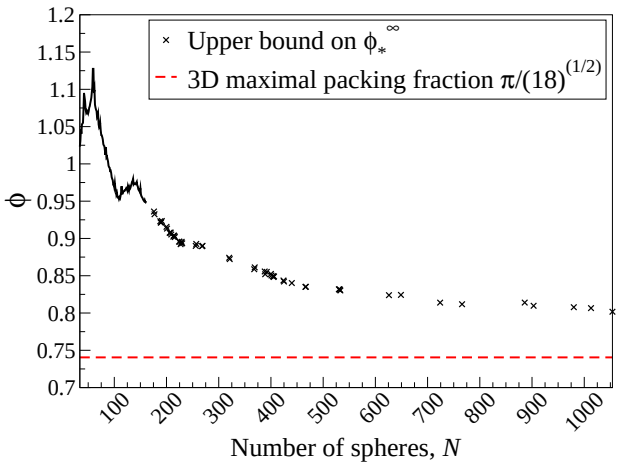

FIG. 3: (Color online) An upper bound on ϕ_*^∞ in $\mathbb{R}^3$ as calculated from the putative $R_{min}(N)$ for $N = 34$ to $N = 161$ and for selected values of $N \geq 176$, versus the (known) maximal packing fraction ϕ_*^∞ of an infinite packing of identical nonoverlapping spheres in $\mathbb{R}^3$, $\phi_*^\infty = \pi/\sqrt{18} \approx 0.7405$.

The upper bound in $\mathbb{R}^3$ (inequality (6), Fig. 3) with maximal local packing fraction $\hat{\phi}_*(N)$ calculated from Eq. (7) converges to ϕ_*^∞ more slowly, as a function of $R_{min}(N)$, than does the upper bound in $\mathbb{R}^2$ [6]. This is intuitive. As the spheres in the bulk of each DLP optimal packing in both $\mathbb{R}^2$ and $\mathbb{R}^3$ at sufficiently large N appear to be packed as the infinite densest packing in their respective space $\mathbb{R}^d$ (this observation is discussed in more detail in Sec. III B), it would be logical to predict that $\hat{\phi}_*(N)$ in the bound (6) converges to ϕ_*^∞ in dimension d roughly as the ratio of sphere surface area to volume, d/R. Up to a small corrective factor that is also dependent on dimension, this appears to be the case, as the

TABLE I: Comparison of $\phi_c(N)$ (8) in $\mathbb{R}^2$ and $\mathbb{R}^3$. The values of $\phi_c(N)$ are compared for $R_{min}(N)$ in $\mathbb{R}^2$ near to $(2/\sqrt{3})R_{min}(N)$ in $\mathbb{R}^3$.

Space	N	$R_{min}(N)$	$(\sqrt{3}/2)R_{min}(N)$	$\phi_c(N)$
$\mathbb{R}^2$	$54-60$	$3.605551-3.830649$		$0.8733-0.9094$
$\mathbb{R}^3$	$530-533$	$4.286296-4.294254$	$3.712041-3.718933$	$0.8785-0.8798$
$\mathbb{R}^2$	$84-88$	$4.581556-4.752754$		$0.9065-0.9312$
$\mathbb{R}^3$	980,1013,1054	$5.334506-5.479129$	$4.619818-4.745065$	$0.9167-0.9236$

following simple model demonstrates.

The maximal local packing fraction $\hat{\phi}_*(N)$ (7) includes in its numerator the total volume of spheres of unit diameter with centers at distance $R_{min}(N)$, even though the (larger) sphere of radius $R_{min}(N)$ whose volume is employed in the denominator does not enclose roughly half of these (smaller) spheres' volume. Approximating the spherical surface of radius $R_{min}(N)$ as a plane, which is a good approximation when the ratio of radii $1/2R_{min}(N)$ is small, a simple model for the volume of the spheres not enclosed by the sphere of radius $R_{min}(N)$ can be built. In this model under the aforementioned approximation, it follows that the d-dimensional spheres of unit diameter in a DLP optimal packing in $\mathbb{R}^d$ with centers on the surface at radius $R_{min}(N)$ should be packed roughly as densely as possible, i.e., with centers arranged as the centers of $(d-1)$-dimensional spheres in the maximally dense packing in $\mathbb{R}^{d-1}$.

Making these two approximations, which become exact in the limit $N \to \infty$, the fraction of the volume of the spheres of unit diameter *not* enclosed by the sphere of radius $R_{min}(N)$ to the volume of the sphere of radius $R_{min}(N)$ is $2/\sqrt{3} \approx 1.155$ times as large in $\mathbb{R}^3$ as in $\mathbb{R}^2$. At any $R_{min}(N)$ for large enough N then, about 15.5% more volume is "added back in" to the numerator of $\hat{\phi}_*(N)$ in $\mathbb{R}^3$ than in $\mathbb{R}^2$, meaning that the convergence fraction,

$$\phi_c(N) \equiv \phi_*^\infty / \hat{\phi}_*(N), \tag{8}$$

at given $R_{min}(N)$ in $\mathbb{R}^3$ should be comparable to the same fraction $\phi_c(N)$ at $(\sqrt{3}/2)R_{min}(N)$ in $\mathbb{R}^2$. This is indeed the case, as is shown in Table I for two ranges of N.

The implications of this relationship are encouraging. Under the two approximations, if the relationship between $\phi_c(N)$ in $\mathbb{R}^3$ and $\mathbb{R}^2$ holds between $\mathbb{R}^d$ and $\mathbb{R}^{d-1}$ for arbitrary d, then a good estimate for ϕ_*^∞ in $\mathbb{R}^d$ can be made. Such an estimate requires knowledge of

ϕ_*^∞ in $\mathbb{R}^{d-1}$ and $\mathbb{R}^{d-2}$ and at least one value of $R_{min}(N)$ for sufficiently large N in $\mathbb{R}^d$. In general, the larger the value of N, the more precise the estimate.

III. COMPARING DLP OPTIMAL PACKINGS TO OPTIMAL SPHERICAL CODES AND BARLOW PACKINGS

In the first part of the following section, we compare DLP optimal packings over the N studied to the densest packings of N nonoverlapping spheres of unit diameter with centers on a spherical surface of radius R, where a configuration of N sphere centers with minimal $R = R_{min}^S$ is sometimes called an optimal spherical code. In the second part of the section, we compare DLP optimal packings to subsets of the densest infinite-volume packings of identical nonoverlapping spheres in $\mathbb{R}^3$, the Barlow packings.

A. Spherical codes and DLP optimal packings

The spatial configurations of spheres in DLP optimal packings can be said to be influenced by several empirical rules, but over the range of N studied, they are dominated by only one. The dominant rule is maximization of the number of spheres on the *surface of the packing*, i.e., the spheres with centers at precisely distance $R_{min}(N)$ from the center of the central sphere. In the vast majority of DLP optimal packings over the range of N studied, this number N_{out} is either the largest or nearly the largest number of spheres whose centers can be placed on a spherical surface of radius $R_{min}(N)$. As N_{out} can take on different values in the general case where there are multiple DLP optimal packings for the same N, we define $N_{out}(N)$ as the maximal number of spheres, from the set of all DLP optimal packings for N spheres, with centers at distance $R_{min}(N)$ from the center of the central sphere. Similarly, we define $N_{out}^{Bar}(N)$ as the maximal number of spheres with centers in the outermost coordination shell at distance $R_{Bar}(N)$ from a central sphere surrounded by a subset of N spheres chosen from a Barlow packing.

The number $N_{out}(N)$ for $R_{min}(N)$ is bounded from above by the number $Z_{max}^S(R_{min}(N))$, where the maximal number of spheres of unit diameter that can be packed with centers on a spherical surface of radius R is termed $Z_{max}^S(R)$. Related to $Z_{max}^S(R)$ is the radius $R_{min}^S(N)$, which we recall is the radius of the smallest spherical surface onto which the centers of N

nonoverlapping spheres of unit diameter can be packed. The problem of finding $Z^S_{max}(R)$ at a given R is a reformulation of the Tammes [21] problem of finding the maximal smallest separation between pairs of points for N points on a sphere of radius unity. The problem of finding $R^S_{min}(N)$ is sometimes called the optimal spherical code problem and has received considerable attention (see, for example, [2]); for $N \leq 130$ and $d = 3$, there are putative solutions to the optimal spherical code problem that are strongly conjectured to be correct [22].

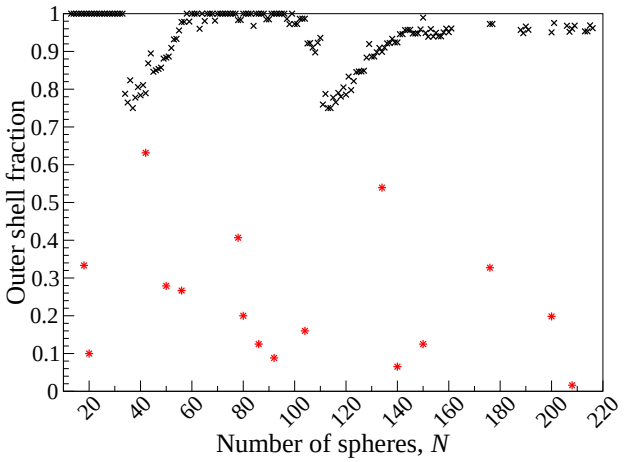

FIG. 4: (Color online) The greatest fraction, number of spheres with centers at distance R over the maximal number that can be packed with centers on a spherical surface of radius R, as compared for all DLP optimal packings at a given N for the N studied from $N = 13$ to $N = 216$ and for subsets of $N + 1$ spheres in any Barlow packing with full coordination shells and the outermost shell at distance $R_{Bar}(N)$. In the figure, a black "X" represents the comparison for DLP optimal packings and a red "*" the comparison for subsets of Barlow packings.

The quantity $N_{out}(N)/Z^S_{max}(R_{min}(N))$ is a measure of the degree to which the surface of a DLP optimal packing is "saturated", where a *saturated surface* of spheres in $\mathbb{R}^d$ is defined as any packing of the maximal number $Z^S_{max}(R)$ of identical nonoverlapping spheres that can be placed with centers at radius R. Using values for $Z^S_{max}(R)$ in $\mathbb{R}^3$ determined from [22] and the DLP optimal packings found by the algorithm, Fig. 4 compares $N_{out}(N)/Z^S_{max}(R_{min}(N))$ and $N^{Bar}_{out}(N)/Z^S_{max}(R_{min}(N))$, respectively, for the N studied from $N = 13$ to $N = 216$ [23] and for N corresponding to full outermost coordination shells of Barlow packings with outermost shells at radii $R_{Bar}(N)$.

For all of the N studied, $N_{out}(N)/Z^S_{max}(R_{min}(N)) \geq 0.75$, and $N_{out}(N) > N^{Bar}_{out}(N)$. Additionally, for 32% of the N in Fig. 4, there is a DLP optimal packing with a saturated surface, i.e., $N_{out}(N) = Z^S_{max}(R_{min}(N))$. These observations indicate that for the N studied,

the densest local packings always include packings with a maximal or near-maximal number of spheres on their surface. Nevertheless, there are also two intervals depicted in Fig. 4 where $N_{out}(N)/Z^S_{max}(R_{min}(N))$ is relatively lower; these intervals coincide with the existence at or near those N of particularly dense DLP optimal packings without saturated surfaces. In these intervals, the bulk of the packing is of more relevance, and the benefits of maximizing the number of spheres on the surface are relatively less advantageous to achieving a densest local packing.

Though the surface-maximization rule is dominant in general, only for $N = 77$ does $R^S_{min}(N_{out}(N)) = R_{min}(N)$. The $N = 77$ DLP optimal packings are therefore the only packings where the precise positions of the spheres *not* on the surface are of no consequence. That is, of $N = 77$ spheres, all 18 not on the surface are rattlers, which is also true for all 24 spheres not on the surface in the $N = 93$ DLP optimal packings. Indeed as N grows large, we have found that the bulk (interior) of each DLP optimal packing begins to resemble a finite subset of one of the Barlow packings, just as in $\mathbb{R}^2$ the bulk of each optimal packing begins to resemble a finite subset of spheres configured with centers on the sites of the triangular lattice.

B. Barlow and DLP optimal packings

As discussed in paper I for large N in $\mathbb{R}^2$, DLP optimal packings can be divided into three regions; the spheres in the bulk that resemble the triangular lattice, the spheres farthest from the center that tend to be configured in circular rings, and those in between the bulk and the surface, which form a sort of "grain boundary." This also appears to be the case in $\mathbb{R}^3$, with the spheres in the bulk of the DLP optimal packings for $N = 766$, 903, 980, 1013 and 1054 closely resembling a subset of the FCC Barlow packing ($N = 903$, 980, 1013, 1054) or resembling a packing that near the central sphere is similar to a subset of the HCP Barlow packing ($N = 766$).

It is of note that the spheres in the bulk of the aforementioned packings are not all placed in *precisely* the same positions as spheres in a subset of a Barlow packing, but instead are within a few percent of the Barlow packing spheres' angular and radial positions as described in spherical coordinates. It is not clear if this continues to be the case for all $N > 1054$, or if for some very large N the bulk of DLP optimal packings are precisely spatially equivalent

to subsets of Barlow packings.

The division of DLP optimal packings at sufficiently large N into three regions is important from the perspective of counting rattlers. For the five N studied where the bulk of the optimal packings closely resemble subsets of Barlow packings, rattlers are present only in the "grain boundary" and surface regions. This suggests that for sufficiently large N, the rattlers in DLP optimal packings are restricted to only these two regions. Consequently, as these regions grow in volume more slowly than the volume of the packing, the ratio of the number of rattlers to the total number of spheres in DLP optimal packings must tend to zero at $N \to \infty$. Further, if the grain boundary region for large enough N does not increase in radial extent with increasing N, then the number of rattlers can grow *at most* in proportion to the surface area of optimal packings. This latter condition appears to be the case for the N studied in both $\mathbb{R}^2$ [6] and $\mathbb{R}^3$.

In $\mathbb{R}^2$, the extent to which the bulk of a DLP optimal packing resembles a packing of contacting disks with centers on the sites of the triangular lattice can be determined visually by perusing an image of the packing. In $\mathbb{R}^3$ however, visual identification is more difficult. To compare the relative extent to which the bulk of DLP optimal packings in $\mathbb{R}^3$ resemble subsets of the Barlow packings, we here introduce the concept of a *similarity metric*, defined as a metric designed to quantify the degree of similarity between one set of points and a reference set.

The subsets of $N+1$ spheres from a Barlow packing with the smallest distance $R_{Bar}(N)$ from the center of the central sphere to any of the surrounding N spheres are not always subsets of the FCC and HCP Barlow packings. This observation suggests that we should compare the DLP optimal packings at various N to reference sets chosen from all Barlow packings, as opposed to only those chosen from the FCC and HCP packings. Therefore, for each N, we define the set of reference sets $\mathbb{B}_N$ as all subsets of $N+1$ spheres chosen from any Barlow packing such that all $N+1$ spheres with centers less than or equal to maximal sphere-distance R from the center of a central sphere are included in the set.

As rigid rotations of DLP optimal packings about the center of the central sphere do not affect packing optimality, we employ a similarity metric that compares only the radial positions of the spheres in an optimal packing to the reference sets. To make this comparison for a DLP optimal packing and a packing from the reference sets at a given N, which we recall are the Barlow packing subsets $\mathbb{B}_N$, $\mathbb{R}^d$ is divided fully into a set $\{\delta_i\}$ of nonoverlapping

spherical shells centered on the center of the reference set's central sphere. Each shell contains within it a number n_i^{ref} of points (sphere centers) from the reference set and a number n_i of sphere centers from the set to be compared. The metric can be written,

$$\mathcal{S} = 1 - \frac{\sum_i |n_i - n_i^{ref}|}{2(N+1)}, \tag{9}$$

where the sum runs over all shells containing at least one point from either set.

For any Barlow packing subset of $N+1$ spheres within a given set $\mathbb{B}_N$, the center of each sphere lies on a coordination shell, where we define the coordination shells locally from the center of only the central sphere. For example, the zeroeth shell is the origin and contains only the center of the central sphere, and the first shell always contains the centers of 12 spheres at distance unity from the origin. To define the radial width of the shells $\{\delta_i\}$ by which the n_i and n_i^{ref} are measured, an average of the radial distances of consecutive coordination shells in the reference packing is used. For example, for an FCC packing with coordination shells at $r = 0, 1, \sqrt{2}, \ldots$, the zeroeth shell is the sphere of radius $(1/2)$ centered at the origin, and the first shell δ_1 of radial width $1/\sqrt{2}$ spans from minor radius $1/2$ to major radius $(1+\sqrt{2})/2$. The final shell can be taken to have infinite width. More detailed information on the reference sets and the choice of the similarity metric defined in Eq. (9) can be found in Appendix B.

Figure 5 plots the greatest similarity metric value from the distinct $\{\delta_i\}$ for all numbers N of spheres studied, along with the greatest similarity metric value for DLP optimal packings for $176 \leq N \leq 1054$ with all spheres with centers at distance $R_{min}(N)$ removed. As is evident from the bottom half of Fig. 5, there is a gradual upward trend in values of $\mathcal{S}$; this is primarily due to the bulk of DLP optimal packings beginning to closely resemble subsets of a Barlow packings for $N \geq 626$, $R_{min}(626) = 4.564905$. In particular, all but one or two of the first 200 spheres in the $N = 766$, 903, 980, 1013 and 1054 optimal packings are arranged in precisely the same first 10 shells $\{\delta_1 \ldots \delta_{10}\}$ as are the spheres that compose one of the $N = 200$ finite subsets of Barlow packings $\mathbb{B}_{200}$.

However, only a few DLP optimal packings for $N \leq 533$, $R_{min}(533) = 4.294254$ bear close resemblance to any of those in the sets $\mathbb{B}_N$. This result is due to the dominance of the empirical rule of surface-maximization in influencing the spatial arrangements of spheres in DLP optimal packings. Simply put, the surface-maximization phenomenon disrupts the

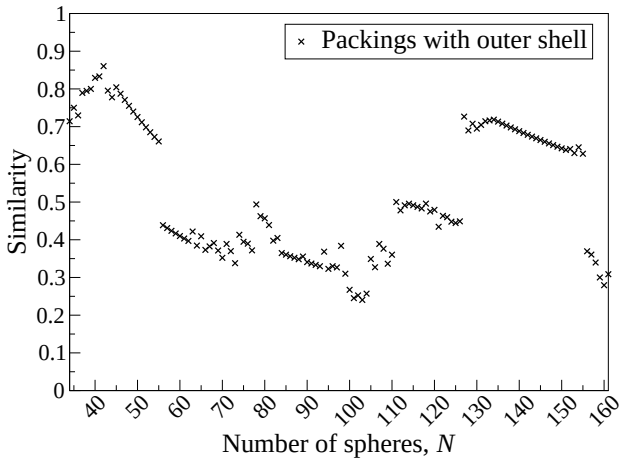

(a)

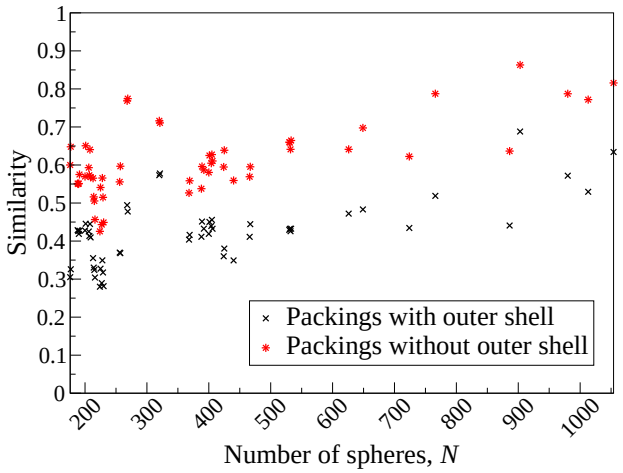

(b)

FIG. 5: (Color online) Similarity metric from (9). An "X" represents the maximal similarity calculated for the comparisons of reference sets $\mathbb{B}_N$ to a DLP optimal packing for N spheres. A "*" represents the maximal similarity for the comparisons of reference sets $\mathbb{B}_M$ to a DLP optimal packing for N spheres with the $N - M$ spheres with centers at distance $R_{min}(N)$ removed.

placement, sufficiently near to the surface, of spheres as subsets of Barlow packings. The range of $R_{min}(N)$ in $\mathbb{R}^3$ over which this disruption is prevalent throughout the entirety of optimal packings is consistent with the same range of $R_{min}(N)$ for DLP optimal packings in $\mathbb{R}^2$, where we compare, as in Table I, values of $(\sqrt{3}/2)R_{min}(N)$ in $\mathbb{R}^3$ to values of $R_{min}(N)$ in $\mathbb{R}^2$. In $\mathbb{R}^2$, signs of the bulk of a DLP optimal packing resembling a triangular lattice packing of contacting disks for consecutive N appear at the earliest around $N = 76$, $R_{min}(76) = 4.417162\ldots$, and do not appear consistently until at least $N \geq 102$, with $R_{min}(102) = 5.166450\ldots$ [6].

Included in the subsets of Barlow packings $\mathbb{B}_N$ are always packings derived from the FCC

and HCP lattices. The former of these is particularly important, as we have found that the highest value of the similarity metric for DLP optimal packings from among the distinct $\{\delta_i\}$ for 169 out of 184, or 91.8% of the $N \geq 34$ that we analyzed, is associated with the FCC-derived packing and its variants indistinguishable to the similarity metric [24], even when $R_{Bar}(N)$ is found from a different packing. This is important, as the FCC-derived packing and its variants indistinguishable to the similarity metric are the packings that, for all N in any set $\mathbb{B}_N$, have the fewest coordination shells.

We have verified for the N studied that the DLP optimal packings *also* consist of shells (of small radial width) containing sphere centers clustered around a relatively low number of radial distances from the center of the central sphere. This is the reason that the highest similarity metric value for all DLP optimal packings chosen from the reference sets in a given $\mathbb{B}_N$ is almost always, for the N studied, associated with the packings that are subsets of an FCC packing: FCC and DLP optimal packings have small numbers of shells.

This characteristic of DLP optimal packings is related to the phenomenon of surface-maximization. The high density of spheres on the surface, due to nonoverlap, requires that the radial separation between the surface spheres and contacting spheres with centers at $r < R_{min}(N)$ be, in general, relatively larger than if the surface contained fewer spheres. Coupled with density-maximization, the rule of surface-maximization drives the spheres for $r < R_{min}(N)$ to cluster around only a few distinct radial positions as well. This observation is reflected in the fact that $\mathcal{S}$ for 48 out of 56, or 85.7% of packings excluding the spheres with centers at $R_{min}(N)$ for $N \geq 176$ are also most similar to the FCC-derived Barlow packing and its variants indistinguishable to the similarity metric. However, the presence of the $N = 766$ packing, which exhibits a bulk that is very similar to a Barlow packing that is not FCC, suggests that this trend may not continue as strongly as N grows larger than $N = 1054$.

Despite that DLP optimal packings for the N studied are generally more radially similar to subsets of FCC than to subsets of other Barlow packings, for $N \leq 533$ they are not angularly similar to any packings in $\mathbb{B}_N$. For optimal packings with high values of $\mathcal{S}$, e.g., for $34 \leq N \leq 55$ and $127 \leq N \leq 155$, the similarity is due entirely to the arrangement of spheres in small numbers of shells, and the DLP optimal packings are more similar to certain dense packings exhibiting icosahedral symmetry. Figure 6, a color-coded representation of the maximal $\mathcal{S}$ from among the reference sets $\mathbb{B}_N$ for $34 \leq N \leq 161$, represents well these

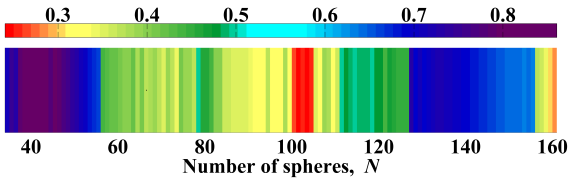

FIG. 6: (Color online) Similarity metric from (9), color-coded as indicated in the key above the diagram, with violet/blue (darker shading) representing the highest values of $\mathcal{S}$ and red/orange (lighter shading) the lowest. The value of $\mathcal{S}$ displayed is calculated as the maximum for DLP optimal packings for a given N compared to the reference sets included in $\mathbb{B}_N$. Due to the similarity between subsets of FCC packings and certain packings with icosahedral symmetry, the ranges of N with highest $\mathcal{S}$, $34 \leq N \leq 55$ and $127 \leq N \leq 155$, are radially and angularly distributed most similarly to a specific, dense packing of spheres with perfect icosahedral symmetry.

regions of icosahedral symmetry. The dense, perfectly icosahedrally symmetric packings to which these DLP optimal packings are similar will be discussed in more detail in Sec. V D.

It is very interesting to note that an FCC arrangement of identical nonoverlapping spheres, in the limit as infinite volume packing fraction $\phi^\infty \to \phi^\infty_* = \pi/\sqrt{18}$, is both the Barlow packing with highest symmetry (cubic) and lowest free energy [25]. Our results state that the densest local packings are most frequently those that are most similar to the maximally dense infinite packing with highest symmetry and lowest free energy even when other packings in $\mathbb{B}_N$ are more locally dense than the FCC-derived packing, i.e., have smaller $R_{Bar}(N)$. As the correspondence in similarity is essentially due to the arrangement of spheres in DLP optimal packings in a relatively small number of shells, this suggests that there is a connection between high symmetry, lowest free energy, and arrangement in a small number of shells in the densest local packings, just as there is between high symmetry, lowest free energy, and arrangement in a small number of shells in the densest infinite packings.

IV. MINIMAL ENERGY AND DLP PROBLEMS

There have been a number of investigations [26–31] into finding arrangements of points that minimize the $12-6$ Lennard-Jones potential with parameters (Eq. 10) $\sigma = 1$, $\epsilon = 1$, a potential possessing features of long-range attraction and strong short range repulsion between pairs of points. The Lennard-Jones potential energy for $N + 1$ points can be

written,

$$V_{LJ}(\mathbf{r}^{N+1}) = 4\epsilon \sum_{1\le i<j\le N+1} \left[\left(\frac{\sigma}{r_{ij}}\right)^{12} - \left(\frac{\sigma}{r_{ij}}\right)^{6} \right], \tag{10}$$

with $r_{ij} \equiv |\mathbf{r}_i - \mathbf{r}_j|$. The known Lennard-Jones minimal-energy (optimal) configurations of $N+1$ points in $\mathbb{R}^3$ can be compared to DLP optimal packings of N spheres around a fixed central sphere of the same size. This comparison is accomplished by scaling the DLP optimal packings such that the minimal distance between sphere centers D is optimized to minimize the Lennard-Jones potential energy given by (10) with $\sigma = 1$, $\epsilon = 1$.

The optimal sphere diameters $D_{opt}(N)$ for $N = 34$ to $N = 161$ lie within a tight range, between $D_{opt}(160) = 1.07953$ and $D_{opt}(44) = 1.09345$, and they average about 1.08319. These diameters may be compared to the Lennard-Jones pair potential minimum, $D = 2^{1/6} \approx 1.12246$. The $D_{opt}(N)$ tend to decrease with increasing N, reflecting a balance obtained as the packing is scaled between the increase in energy due to spheres in contact at distance $D_{opt}(N) < 2^{1/6}$ and the decrease in energy obtained by all other spheres at distances greater than $2^{1/6}$. Comparing DLP and Lennard-Jones optimal configurations for the same number of points (sphere centers), we find that sets of optimal packings only overlap for the trivial cases $N = 1$ and $N = 2$; in general, they are completely different, with the V_{LJ} of the DLP optimal packings with optimized D for $N = 34$ to $N = 161$ about $80\% - 95\%$ of the minimal known V_{LJ} for $N+1$ points. Figure 7 depicts the minimal V_{LJ} alongside the V_{LJ} of DLP optimal packings with optimized $D_{opt}(N)$ for $N = 34$ to $N = 161$.

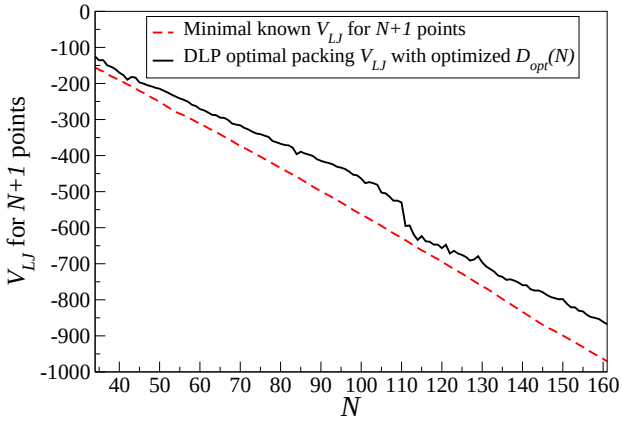

FIG. 7: (Color online) Plot of the minimum known [31] $V_{LJ}(\mathbf{r}^{N+1})$ (10) for $N+1$ points vs the V_{LJ} of DLP optimal packings with spheres of optimized diameter $D_{opt}(N)$ for $N = 34$ to $N = 161$.

In Fig. 7, there are several N for which V_{LJ} for the DLP optimal packings and the optimal

configurations of $N+1$ points with Lennard-Jones potential (10) are relatively closer [32]. They are particularly close for three ranges of N centered around $N = 42$, 114, and 134, points that are local minima in the percent difference between the two V_{LJ}. The proximity of the V_{LJ} around these N can be attributed to the symmetry of the DLP optimal packings at these three N, and to the spatial similarities between DLP optimal packings for these three N and the packings for N in small ranges around these three. It is known [27, 29] that minimal-energy configurations of points with Lennard-Jones potential tend to favor icosahedral symmetry, either in part of the configuration or in its entirety. The $N = 42$ and $N = 134$ DLP optimal packings are similarly roughly icosahedrally symmetric, and though the $N = 114$ DLP optimal packing exhibits perfect three-fold rotational (chiral) symmetry, its first and last shells are also roughly icosahedrally symmetric.

Another minimal-energy problem involves finding the minimal-energy (optimal) spatial configurations of $N+1$ identical nonoverlapping spheres where potential energy V_{sm} is defined in terms of the second moment about the centroid of the $N+1$ sphere centers,

$$V_{sm}(\mathbf{r}^{N+1}) = \sum_{i=1}^{N+1} |\mathbf{r}_i - \mathbf{C}|^2, \tag{11}$$

with $\mathbf{C} \equiv (N+1)^{-1} \sum_{i=i}^{N+1} \mathbf{r}_i$ the centroid [33]. Comparing DLP and minimal second moment optimal packings up to $N = 32$, the largest N for which minimal second moment optimal packings are available, we find that only for $N = 1$ to $N = 4$ do sets of optimal packings overlap, and as with the Lennard-Jones problem, in general they are completely different.

The wide variance in optimal configurations at the same number of spheres (points) across minimal-energy problems has implications for nucleation theory. Comparing these three problems, we see that the functional form of the potential energy has a substantial effect on the spatial arrangement of optimal configurations, despite that the potentials in all three problems are isotropic with long-range attractions and strong short-range repulsions. This suggests that the sizes and shapes of critical nuclei in classical overcompressed liquids (where dynamics are generally dominated by strong short-range repulsion) may depend heavily on the precise functional form of the pair potential acting between particles. The potential effects of the structures of dense nuclei on the probability of freezing in overcompressed liquids will be discussed in further detail in Sec. VI.

V. DLP OPTIMAL PACKINGS IN THREE DIMENSIONS

Despite that the DLP optimal packings are almost always most similar, from among the packings in $\mathbb{B}_N$, to a subset of an FCC Barlow packing or one of its variants indistinguishable to the similarity metric, all optimal packings with $N \geq 13$ are significantly more locally dense than any subset of a Barlow packing including $N+1$ spheres. In general, over the range of N studied in $\mathbb{R}^3$, we find wide variation in the symmetries, contact networks, and other characteristics of DLP optimal packings, just as in $\mathbb{R}^2$.

For the majority of N, there are an uncountably infinite number (a continuum) of DLP optimal packings with optimal radius $R_{min}(N)$, with the continuum attributable to the presence of rattlers. Over the 184 DLP optimal packings studied between $N = 34$ and $N = 1054$, not including the central sphere, 170 contain rattlers (identified to the same precision in spatial coordinates as the coordinates in the packing), with every packing for $N > 114$ containing at least one rattler.

In the following figures (Figs. 8-18), only the backbones, or the packings with the rattlers removed, are depicted, unless otherwise specified. Additionally, each DLP packing is divided into shells, where a shell in a DLP optimal packing is defined as all spheres with centers at an equal distance R from the center of the central sphere. Each shell can be visualized in the plane by employing a mapping to project points on a spherical surface in $\mathbb{R}^3$ (a shell) to a disk of radius π in $\mathbb{R}^2$. Considering a point in $\mathbb{R}^3$ in spherical coordinates and a point in $\mathbb{R}^2$ in polar coordinates, the mapping leaves the azimuthal angle unchanged while the angle of inclination in $\mathbb{R}^3$ becomes the radius in $\mathbb{R}^2$. The zenith direction from which the angle of inclination is measured is generally selected to preserve angular symmetry. In Figs. 8-18, points of distance unity (contacting spheres) in $\mathbb{R}^3$ are joined by lines.

A. DLP optimal packings for $N \leq 33$

In $\mathbb{R}^d$ for any d, all DLP optimal packings with $N \leq K_d$ the kissing number have $R_{min}(N) = 1$, with $K_3 = 12$ in $\mathbb{R}^3$. Also for any d, the set of all DLP optimal packings for a given N with $R_{min}(N) \leq \tau$, $\tau = (1+\sqrt{5})/2$ the golden ratio, include configurations where all N sphere centers lie on a spherical surface of radius $R_{min}(N) = R^S_{min}(N)$ [1]. We recall that $R^S_{min}(N)$ is the radius of the smallest spherical surface onto which the centers of

N spheres of unit diameter can be packed. The greatest N for which $R_{min}(N) \leq \tau$, denoted by N_d^τ, in $\mathbb{R}^3$ is $N_3^\tau = 33$. For $13 \leq N \leq 33$ in $\mathbb{R}^3$, our findings indicate that there are no DLP optimal packings with jammed spheres with centers at a radius $r < R_{min}(N)$.

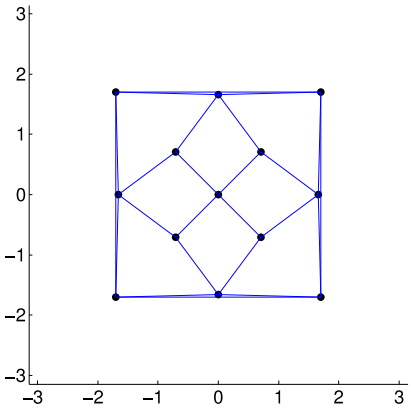

(a)

FIG. 8: (Color online) This plot is a projection from the surface of a sphere of radius $R_{min}(13) = 1.045573\ldots$ of 13 points (sphere centers) in $\mathbb{R}^3$ to the interval $[-\pi, \pi] \times [-\pi, \pi]$ in $\mathbb{R}^2$. As the projection to $\mathbb{R}^2$ is most clearly defined in terms of polar coordinates and does not preserve distances from $\mathbb{R}^3$, we do not provide labels for our axes. This DLP optimal packing contains only a single shell, the sphere centers of which belong to point group C_4. In the projection, the angle of inclination of a point in $\mathbb{R}^3$ represented in spherical coordinates becomes the distance from the origin (radius) in $\mathbb{R}^2$, while the azimuthal angle remains unchanged. Contacting spheres, i.e., spheres with centers (points) in $\mathbb{R}^3$ separated by unit distance where all spheres are of unit diameter, are connected by straight lines in the plot in $\mathbb{R}^2$. The zenith direction from which each point's (sphere center's) angle of inclination is measured is chosen to coincide with the packing's C_4 axis; in this way, the projection to the plane preserves the rotational symmetry of the packing in $\mathbb{R}^3$ about the C_4 axis.

Figure 8 is a projection to $\mathbb{R}^2$ of the $N = 13$ DLP optimal packing found by the algorithm. This configuration of spheres was first documented in [5], where the authors conjectured that it was the densest packing of 13 nonoverlapping spheres of unit diameter with centers restricted to a spherical surface of radius R. According to the principle (proved in Ref. [1]) that for $K_d < N \leq N_d^\tau$, $R_{min}(N) = R_{min}^S(N)$, we conjecture that it is also the densest packing, without restriction, of 13 spheres around a fixed central sphere.

Unlike in $\mathbb{R}^2$, we know of no rigorous proofs indicating for $K_3 < N \leq N_3^\tau$ what are the smallest radii R, equal to $R_{min}(N)$, onto which the centers of N identical nonoverlapping spheres of unit diameter may be placed. However, we have found that the putative $R_{min}(N)$ found by the algorithm for $13 \leq N \leq 33$ are equal to the strongly conjectured values for $R_{min}^S(N)$ presented in [22]. This provides further evidence that these smallest-known

$R^S_{min}(N) = R_{min}(N)$ are optimal.

B. Particularly dense, symmetric optimal packings

For four values of N, $N = 60, 62, 84$ and 114, a highly symmetric arrangement of spheres yields a packing that is significantly more locally dense than DLP optimal packings of nearby N. The relatively high densities of these packings appears in Fig. 1 as upturns above the linear trend and in Fig. 2 as downturns below the one-third power (in N) trend. All N surrounding spheres in each of these four packings are locally jammed, though in two of the four cases, the central sphere is not in contact with any of its nearest neighbors (which would make the central sphere a rattler were it not fixed).

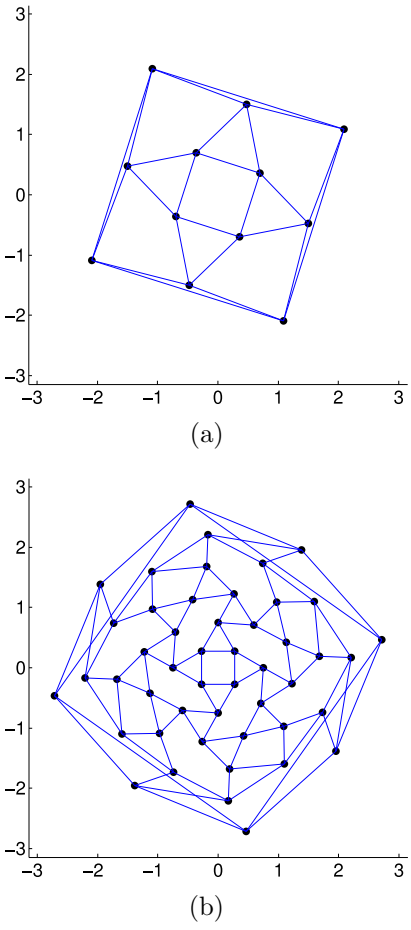

FIG. 9: (Color online) As in Fig. 8, except here we show the two shells of the $N = 60$ DLP optimal packing, which belongs to point group O. The zenith direction is chosen along one of the C_4 axes shared by both shells. (a) 12 spheres, $R = 1$, point group O_h. (b) 48 spheres, $R = R_{min}(60) = 1.891101\ldots$, point group O.

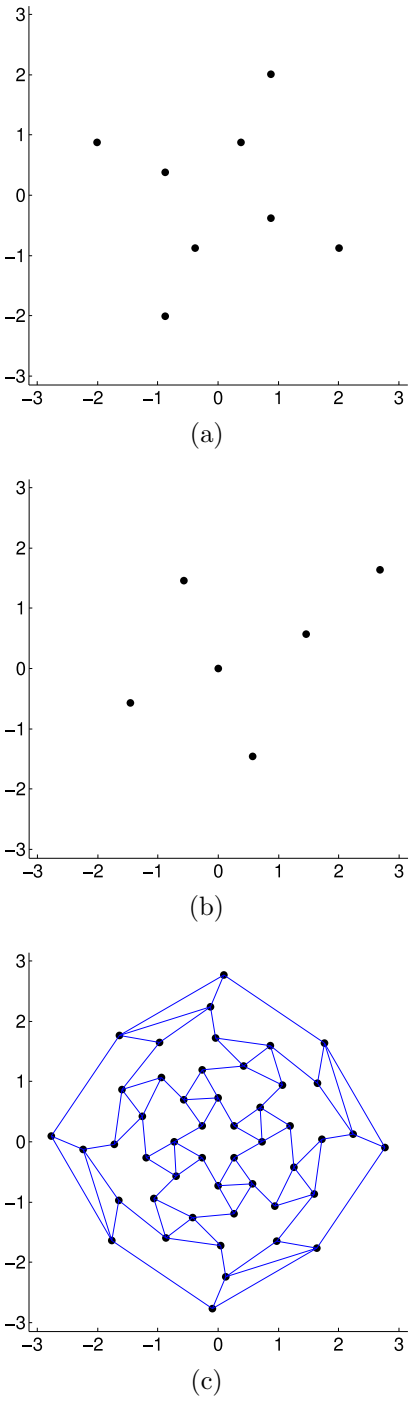

FIG. 10: (Color online) As in Fig. 8, except here we show the three shells of the $N = 62$ DLP optimal packing, which belongs to point group O. The zenith direction is chosen along one of the C_4 axes shared by all three shells. (a) 8 spheres, $R = 1.087542\ldots$, point group O_h. (b) 6 spheres, $R = 1.087786\ldots$, point group O_h. In this projection, as the sphere center furthest from the origin is at distance π (corresponding in $\mathbb{R}^3$ to an angle of inclination equal to π), its azimuthal angle is chosen at random. (c) $R = R_{min}(62) = 1.927716\ldots$, point group O.

Figure 9 depicts the two shells of the $N = 60$ DLP optimal packing, which has rotational

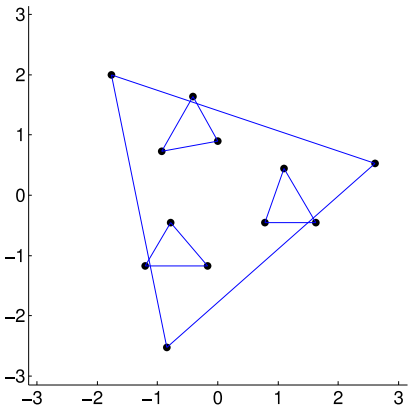

(a)

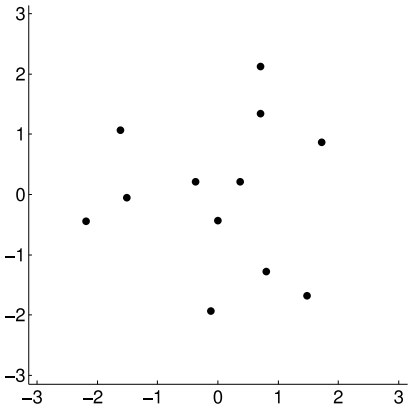

(b)

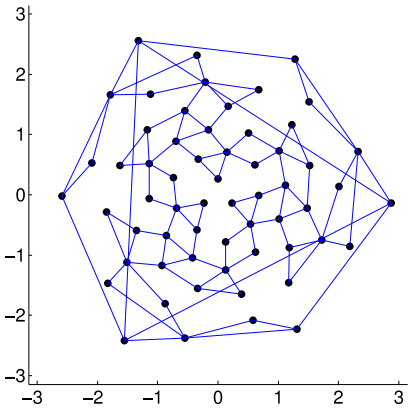

(c)

FIG. 11: (Color online) As in Fig. 8, except here we show the three shells of the $N = 84$ DLP optimal packing, which belongs to point group T. The zenith direction is chosen along one of the C_3 axes shared by all three shells. (a) 12 spheres, $R = 1.255451\ldots$, point group T. (b) 12 spheres, $R = 1.423714\ldots$, point group T. (c) 60 spheres, $R = R_{min}(84) = 2.182390\ldots$, point group T.

(chiral) octahedral symmetry. The first shell contains 12 spheres (the zeroeth shell is the central sphere) arranged with full octahedral symmetry and in contact with the central

sphere. The second shell contains 48 spheres with rotational octahedral symmetry and with centers at distance $R_{min}(60) = 1.891101\ldots$. It is of note that the $N = 60$ optimal packing is such a relatively densely-packed configuration of spheres that $R_{min}(59) = R_{min}(60)$, and DLP optimal packings for $N = 59$ can be formed simply by deleting any one of the 60 surrounding spheres in the $N = 60$ packing.

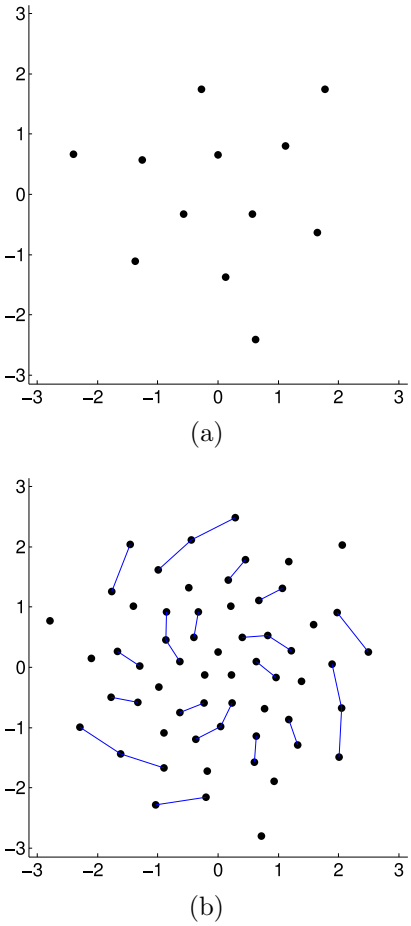

FIG. 12: (Color online) As in Fig. 8, except here we show the first and tenth shells of the $N = 114$ DLP optimal packing, which has ten shells and belongs to point group D_3. The zenith direction is chosen along one of the C_3 axes shared by all ten shells. (a) 12 spheres, $R = 1$, point group D_3. (b) 60 spheres, $R = R_{min}(114) = 2.456227\ldots$, point group D_3.

Figure 10 depicts the three shells of the $N = 62$ DLP optimal packing. The shells contain 8, 6, and 48 spheres, respectively, at distances $R = 1.087542\ldots$, $R = 1.087786\ldots$ and $R_{min}(62) = 1.927716\ldots$ from the center of the central sphere. The first and second shell have full octahedral symmetry, while the third and the packing as a whole exhibit only rotational octahedral symmetry. The first and second layers of the $N = 62$ packing are radially less than 2.5×10^{-4} sphere diameters from one another, and together they form a

cavity within which the central sphere, were it not fixed, could move. This effect also occurs with disks in $\mathbb{R}^2$, as is discussed in paper I [36]. More detail on this topic is presented in Sec. V F.

Figure 11 shows the three shells of the $N = 84$ DLP optimal packing, all of which have rotational tetrahedral symmetry. The shells contain 12, 12, and 60 spheres, respectively, at distances $R = 1.255451\ldots$, $R = 1.423714\ldots$, and $R_{min}(84) = 2.182390\ldots$ from the center of the central sphere. The $N = 84$ DLP optimal packing is unique in that it is the only optimal packing that we have found, in $\mathbb{R}^2$ or $\mathbb{R}^3$, that exhibits perfect tetrahedral symmetry.

The $N = 114$ DLP optimal packing is composed of ten shells. The first includes 12 spheres in contact with the central sphere, and the tenth 60 spheres at $R_{min}(114) = 2.456227\ldots$; both have chiral three-fold dihedral symmetry. Shells two and six each contain three spheres with centers arranged as an equilateral triangle (point group D_{3h}), and shells three through five and seven through nine each contain six spheres arranged with chiral three-fold dihedral symmetry. Shells two through nine can be grouped into four pairs based on radial distance from the central sphere. Each pair is no more than 2.22×10^{-3} sphere diameters apart (shells two and three), but at least 1.24×10^{-6} sphere diameters apart (shells eight and nine). Figure 12 is an image of shells one and ten.

C. Other optimal packings with high symmetry

Over the N studied, a large number of DLP optimal packings were found, aside from those discussed in Sec. V B, that exhibit perfect symmetry. A representative selection of these packings is presented in this section.

Figure 13 depicts the last shells in the optimal packings for $N = 45$ and $N = 57$ spheres; both packings have three-fold cyclic symmetry (point group C_3). Also in both packings, all spheres including the central sphere are jammed. The $N = 45$ packing has four shells containing 6, 3, 3, and 33 spheres with centers at radial distance $R = 1$, $R = 1.005960\ldots$, $R = 1.032049\ldots$, while $R_{min}(45) = 1.749670\ldots$, respectively. The $N = 57$ packing has three shells containing 9, 3, and 45 spheres with centers at radial distance $R = 1$, $R = 1.009196\ldots$, and $R_{min}(57) = 1.877196\ldots$, respectively.

Neither the $N = 61$ nor the $N = 74$ optimal packings are perfectly symmetric; both belong to point group C_1. However, with one sphere removed, the remaining 61 spheres of

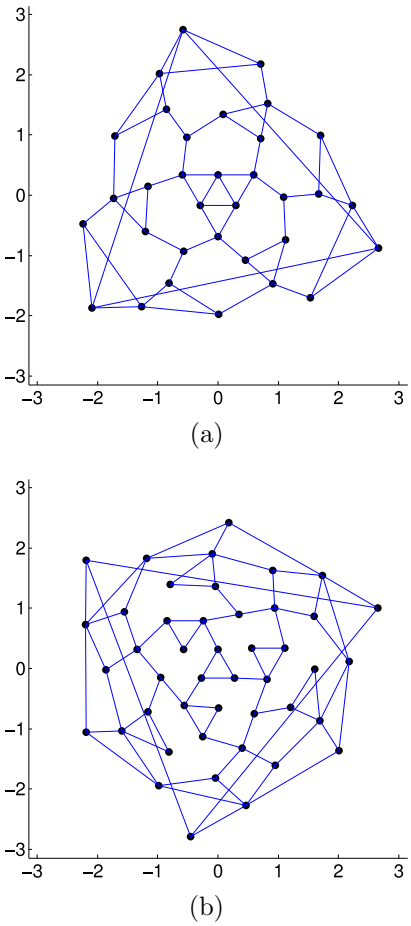

FIG. 13: (Color online) As in Fig. 8, except here we show the last shells of the $N = 45$ and $N = 57$ DLP optimal packings, both of which belong to point group C_3. For both shells, the zenith direction is chosen along one of the C_3 axes shared by all shells in the packing. (a) 33 spheres, $R = R_{min}(45) = 1.749670\ldots$, point group C_3. (b) 45 spheres, $R = R_{min}(57) = 1.877196\ldots$, point group C_3.

the $N = 61$ packing have four-fold cyclic symmetry (point group C_4), and with two jammed spheres and four rattlers (from the last shell) removed, the remaining 69 spheres of the $N = 74$ packing also have four-fold cyclic symmetry. Figure 14 is an image of the jammed spheres in the last shells in the $N = 61$ and $N = 74$ DLP optimal packings. Neither packing has a jammed central sphere.

Figure 15 is an image of the eighth and last shell of the $N = 50$ DLP optimal packing; the shell contains 35 jammed spheres with centers at radial distance $R_{min}(50) = 1.814049\ldots$ from the center of the central sphere. The first three shells form a cavity around the central sphere and contain four, two, and two spheres with centers at radial distances $R = 1$, $R = 1.000608\ldots$, and $R = 1.037107\ldots$, respectively. The fourth through seventh shells are

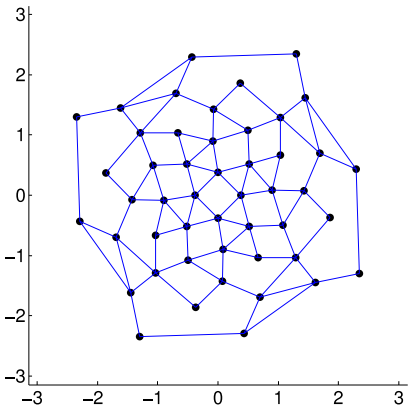

(a)

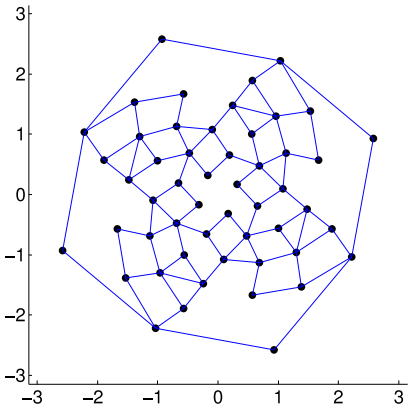

(b)

FIG. 14: (Color online) As in Fig. 8, except here we show the jammed spheres in the last shells of the $N = 61$ and $N = 74$ DLP optimal packings, both of which belong to point group C_4. For both shells, the zenith direction is chosen along one of the C_4 axes. (a) 48 spheres, $R = R_{min}(61) = 1.919927\ldots$, point group C_4. (b) 52 jammed spheres (of 56 total in the shell), $R = R_{min}(74) = 2.077792\ldots$, point group C_4.

single spheres positioned at distances $1.108 < R < 1.151$, and the 35 jammed spheres in the eighth shell are arranged with mirror reflection symmetry (point group C_s). The $N = 50$ packing is a particularly good example of the complicated structures resulting from many-bodied interactions in DLP optimal packings, in that it is not symmetric as a whole (point group C_1) but contains shells exhibiting perfect symmetry that does not appear related to the geometry of a spherical surface. It is also interesting to note that the eighth shell of the $N = 50$ DLP optimal packing is the *only* example for $N \geq 34$ in $\mathbb{R}^3$ of an achiral last shell, i.e., it is the only last shell exhibiting a plane of reflection symmetry.

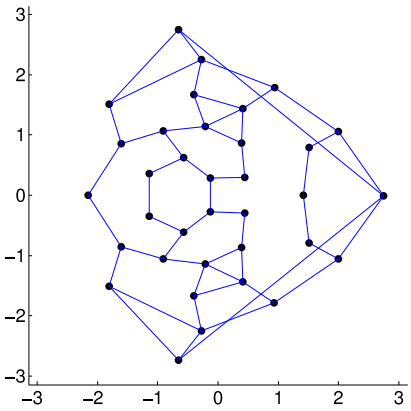

FIG. 15: (Color online) As in Fig. 8, except here we show the last shell of the $N = 50$ DLP optimal packing, which contains 35 jammed spheres with centers at distance $R_{min}(50) = 1.814049\ldots$ and belongs to point group C_s. The zenith direction in the image is chosen parallel to the mirror plane and through the contact point of two spheres.

D. Imperfect icosahedral symmetry in DLP optimal packings

Perhaps equally as interesting as the DLP optimal packings in $\mathbb{R}^3$ that are perfectly symmetric are those packings that exhibit only rough or imperfect symmetry. For example, no single shell in a DLP optimal packing over the N studied exhibits perfect five-fold rotational or higher symmetry; in particular, no shell exhibits perfect icosahedral symmetry. This is not the case in $\mathbb{R}^2$, where there are three DLP optimal packings (for $N = 10$, $N = 15$ and $N = 25$) with perfect five-fold rotational symmetry, and a large number with perfect six-fold rotational symmetry.

In $\mathbb{R}^2$, the kissing number $K_2 = 6$, and there is only one way (up to rotations) to arrange six identical disks in contact with a same-size central disk: each of the six must contact two of the remaining five, such that the arrangement enclosed in an encompassing disk is jammed. It is therefore not particularly surprising that six-fold rotational symmetry is common in DLP optimal packings in $\mathbb{R}^2$. In $\mathbb{R}^3$, the kissing number $K_3 = 12$, but there is an infinite number of ways to arrange 12 identical spheres in contact with a same-size central sphere.

The differences between configurations of K_d spheres in contact with the central sphere in dimensions two and three can serve as an explanation for why perfect icosahedral symmetry is not found, over the N studied, in the DLP optimal packings in $\mathbb{R}^3$. In $\mathbb{R}^3$, the central sphere contributes to the disruption of perfect icosahedral symmetry by preventing the 12 surrounding spheres from forming an icosahedron of contacting spheres, as 12 identical

TABLE II: Details of a dense, perfectly icosahedrally symmetric packing of 134 identical nonoverlapping spheres around a same-size central sphere.

Shell	Spheres	Shape	Side length	Exact vertex distance	Num. vertex distance
1	12	icosahedron	$\frac{2}{(\tau+2)^{1/2}}$	1	1
2	30	icosidodecahedron	$\frac{2}{(\tau+2)^{1/2}}$	$\frac{2\tau}{(\tau+2)^{1/2}}$	1.701302...
3	12	icosahedron	$\frac{4}{(\tau+2)^{1/2}}$	2	2
4	80	truncated icosahedron	$\frac{2}{(\tau+2)^{1/2}}$	$\left(\frac{9\tau+10}{\tau+2}\right)^{1/2}$	2.605543...

contacting spheres with centers on the vertices of an icosahedron is the densest packing of 12 spheres around a point.

Supporting this explanation, imperfect icosahedral symmetry is present in a significant number of the first shells in DLP optimal packings. Specifically, if the tolerance for sphere center overlap used in calculating symmetry elements is raised from 10^{-8} to 0.2 sphere diameters, then the 12 spheres in contact with the central sphere in the first shells of the DLP optimal packings for the $N = 42$, $N = 114$, 116, 117, 118, 133, 135$-$139, and 530$-$532 DLP optimal packings all exhibit icosahedral symmetry. Additionally, the 12 spheres closest to the central sphere in the $N = 269$, 320, 533, and 886 packings exhibit icosahedral symmetry within a tolerance of 0.2 sphere diameters.

Imperfect icosahedral symmetry is present in many DLP optimal packings at radial distances much greater than unity. In general, for N near $N = 42$ and $N = 134$, DLP optimal packings exhibit imperfect icosahedral symmetry throughout the entire packing. This is due to the existence of two particularly dense, perfectly icosahedrally symmetric packings containing two and four shells, respectively, totaling 42 and 134 identical nonoverlapping spheres surrounding a central same-size sphere. The first 134 spheres in the $N = 269$, 320, and 530$-$533 DLP optimal packings can be described as variations on the 134-sphere packing, which contains as a subset the 42-sphere packing. Table II provides the details of the polyhedra composing the perfectly symmetric 134-sphere packing, where the fourth shell of the packing includes 60 spheres with centers on the vertices of a truncated icosahedron and an additional 20 spheres with centers arranged along radial vectors from the center of the packing through the centers of each of the truncated icosahedron's 20 regular hexagonal faces.

The numbers of spheres in the outer shells of the two perfectly icosahedrally symmetric

packings are near to the maximal number $Z^S_{max}(R_{min}(N))$ that can be placed on spherical surfaces of radii $R_{min}(42)$ and $R_{min}(134)$, respectively. As a result, DLP optimal packings at N near 42 and 134 can be packed similarly to these icosahedrally symmetric packings while roughly adhering to the empirical rule of surface-maximization. However, none of the spheres in any of the perfectly icosahedrally symmetric packing's shells are in contact with any other spheres within that shell, and the spheres in the second icosahedron (third shell) are not in contact with any of the spheres in the icosidodecahedron (second shell). This lack of contact allows the spheres to be translated away from their perfectly icosahedrally symmetric positions in order to obtain a smaller DLP optimal packing radius $R_{min}(N)$ for N near $N = 42$ and $N = 134$.

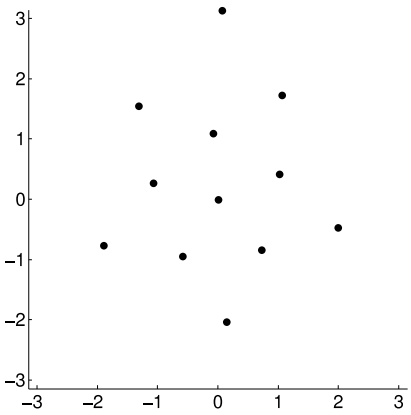

(a)

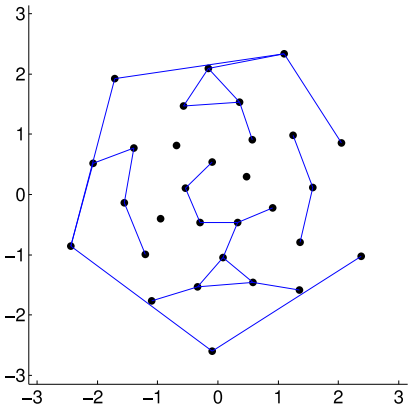

(b)

FIG. 16: (Color online) As in Fig. 8, except here we show the two shells of the $N = 42$ DLP optimal packing; the 12 sphere centers of the first shell roughly form the vertices an icosahedron, and the 30 sphere centers (including 3 rattlers) of the second shell roughly form the vertices a icosidodecahedron. The zenith direction in both cases is chosen along one of the rough C_5 axes. (a) 12 spheres, $R = 1$, point group I_h (to 0.012 sphere diameters). (b) 30 spheres, $R_{min}(42) = 1.699423\ldots$, point group I_h (to 0.195 sphere diameters).

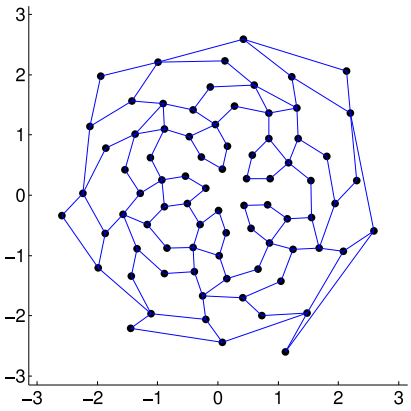

(a)

FIG. 17: (Color online) As in Fig. 8, except here we show the last shell of the roughly icosahedrally symmetric $N = 134$ DLP optimal packing, including 80 spheres with centers at distance $R_{min}(134) = 2.585816\ldots$. The centers of 60 of the spheres roughly form the vertices of a truncated icosahedron, while the remaining 20 spheres are centered in the truncated icosahedron's hexagonal faces. The zenith direction is chosen along one of the rough C_5 axes.

The two shells of the $N = 42$ DLP optimal packing are depicted in Fig. 16, where the shells contain 12 and 30 spheres, respectively, just as do the shells of the dense icosahedrally symmetric packing described in the first two rows of Table II. The variation on the two perfectly icosahedrally symmetric polyhedra that form the $N = 42$ DLP optimal packing achieves an improvement of 0.001879 sphere diameters in R, with $R_{min}(42) = 1.699423\ldots$. The last shell of the $N = 134$ DLP optimal is depicted in Fig. 17. The $N = 134$ packing includes; 12 spheres within radial distances 1 and 1.036, 30 within radial distances 1.637 and 1.763, 12 (of which five are rattlers) within radial distances 1.999 and 2.036 (icosahedrally symmetric to 0.075 sphere diameters), and 80 at exactly $R_{min}(134) = 2.585816\ldots$. The DLP optimal packing for $N = 134$ achieves an improvement of $0.0197270\ldots$ over the perfectly icosahedrally symmetric packing.

E. Maracas packings

In a spherical region, the most area available to place the centers of nonoverlapping spheres is on the surface. Consequently, is is perhaps expected that DLP optimal packings would contain saturated or nearly saturated surfaces. However, it is surprising that the salient features of certain DLP optimal packings are entirely determined by the distribution of the spheres with centers at precisely radius $R_{min}(N)$.

The DLP optimal packings for $N = 77$ and $N = 93$ are termed "maracas" packings; they are perfect examples of the phenomenon of surface-maximization, and exhibit some of the lowest values of the greatest $\mathcal{S}$ compared, respectively, to the packings in the sets $\mathbb{B}_{77}$ and $\mathbb{B}_{93}$. The maracas packings each consist of a few unjammed spheres free to rattle within a "husk" composed of the maximal number of spheres that can be packed with centers at $R_{min}(N)$. Further, $R_{min}(77) = R^S_{min}(N_{out}(77))$ and $R_{min}(93)$ is only $6.606796\cdots \times 10^{-5}$ sphere diameters larger than $R^S_{min}(N_{out}(93))$. Figure 18 depicts the first and only shells for the maracas packings.

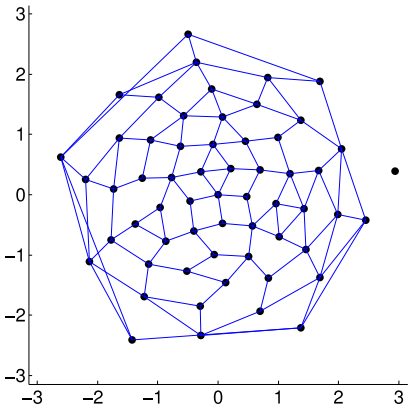

(a)

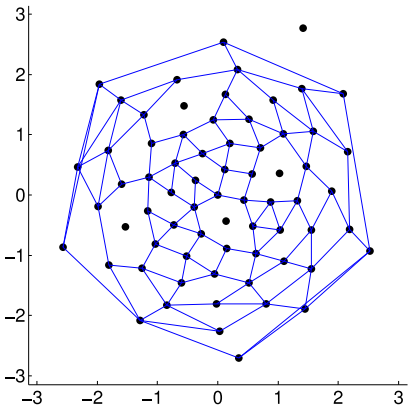

(b)

FIG. 18: (Color online) As in Fig. 8, except here we show the first and only shells for the $N = 77$ and $N = 93$ "maracas" packings, including rattlers. The zenith direction in each case is chosen somewhat arbitrarily to run through the center of one of the surrounding spheres. (a) 59 spheres, one rattler, $R_{min}(77) = 2.111526\ldots$, point group C_1. (b) 69 spheres, five rattlers, $R = R_{min}(93) = 2.280243\ldots$, point group C_1.

F. Optimal packings where the central sphere is not locally jammed

As in $\mathbb{R}^2$, for small enough N, there are many DLP optimal packings in $\mathbb{R}^3$ where a number of jammed spheres form a cavity around the central sphere such that were the central sphere not fixed, it would be a rattler. The $N = 62$ packing already discussed exhibits this characteristic, containing eight spheres with centers at $R = 1.087542\ldots$ and six with centers at $R = 1.087786\ldots$ from the center of the central sphere. The $N = 61$ packing has a similar cavity composed of three layers of four spheres each with centers at respective distances $R = 1.013330\ldots$, $R = 1.028826\ldots$, and $R = 1.019676\ldots$, configured as squares. The $N = 74$ optimal packing exhibits a cavity composed of four layers of four spheres each with centers configured as squares and at respective distances $R = 1.152237\ldots$, $R = 1.156068\ldots$, $R = 1.167618\ldots$, and $R = 1.225331\ldots$. The cavities around the central sphere in the $N = 73$ and $N = 78$ packings are composed of ten layers and nine layers, respectively, of two spheres each.

The cavities formed are not, however, always symmetric. For 59 of the 184 N studied, DLP optimal packings were found containing cavities such that the center of the nearest sphere to the central sphere was at distance $R > 1$; for only seven of these is any layer composed of more than one sphere.

In general, the cavities range in number of spheres from 8 for $N = 50$ to 26 for $N = 99$. The center of the first sphere forming the cavity ranges from distance $R = 1.006188\ldots$ for $N = 154$ to $R = 1.356622\ldots$ for $N = 99$. The farthest of the 26 spheres forming the cavity in the $N = 99$ DLP optimal packing has center at distance $R = 1.537500\ldots$, indicating that the volume of space available in the cavity to the center of the central sphere is more than three times the sphere's volume.

VI. CONCLUSIONS

DLP optimal packings in $\mathbb{R}^3$ are widely spatially diverse and differ, particularly on the surface, from subsets of the Barlow packings at all N. They sometimes display elements of perfect symmetry and often display elements of imperfect symmetry, such as imperfect icosahedral symmetry for sufficiently small N. They are similar in these respects to DLP optimal packings in $\mathbb{R}^2$, which differ from packings of contacting disks with centers on the

vertices of the triangular lattice. However, at sufficiently large values of N in any $\mathbb{R}^d$, the bulk of DLP optimal packings must begin to closely resemble a subset of one of the densest infinite packings in respective $\mathbb{R}^d$ or fail to be a densest local packing.

In $\mathbb{R}^3$, optimal packings tend to have a minimum number of shells and a last shell that is almost always nearly saturated (or saturated). These features lead to DLP optimal packings most closely resembling, as measured by a scalar similarity metric (9), subsets of Barlow packings consisting of $N+1$ spheres (a packing in $\mathbb{B}_N$) with the same distribution of coordination shells as an FCC packing.

Knowledge of $R_{min}(N)$ for certain $N = N_*$ in $\mathbb{R}^d$ makes possible the construction of a rigorous upper bound (6) on the maximal density of an infinite sphere packing in $\mathbb{R}^d$; this bound becomes more restrictive as N_* grows large, and becomes the equality $\hat{\phi}_*(N_*) = \phi_*^\infty$ as $N \to \infty$. Knowledge of the $R_{min}(N)$ also makes possible the construction of a function $Z_{max}(R)$ that is an upper bound (2) on the expected number of sphere centers $Z(R)$ within distance R from any given sphere center, which can be related to a packing's pair correlation function $g_2(r)$ in $\mathbb{R}^3$ by (3). This upper bound is a realizability condition on a candidate pair correlation function $g_2(r)$ for a packing of spheres, similar to the nonnegativity conditions on $g_2(r)$ and its corresponding structure factor $S(k)$.

The function $Z_{max}(R)$ is also a significantly more restrictive upper bound on candidate cross-correlation functions for a packing of a special central sphere and its surrounding spheres, say, a single spherical solute molecule that attracts same-size spherical solvent molecules. The critical distinction between a cross-correlation function for a single sphere and a system-wide pair correlation function $g_2(r)$ is that $g_2(r)$ is an expected value or average over all identical spheres in a packing, whereas a cross-correlation function for a single sphere applies locally, just as the function $Z_{max}(R)$ is derived locally.

Considering, for example, the spheres forming the cavity wall in DLP optimal packings in $\mathbb{R}^3$ with cavities around the central sphere, it is clear that not every sphere in a packing can have the maximal number $Z_{max}(R)$ of sphere centers within distance R from its center (except for R such that $Z_{max}(R) = 12$, where the Barlow packings realize this criterion). However, as any single (solute) sphere can have the maximal number of (solvent) sphere centers within distance R from its center, a $Z(R)$ defined in terms of a cross-correlation function of a single central sphere can be equal to $Z_{max}(R)$ at any R. Otherwise expressed, for $g_2^{yz}(r)$ any realizable cross-correlation function between nonoverlapping spherical solute

molecules of unit diameter (of type y) in the dilute limit and same-size spherical solvent molecules (of type z),

$$Z_{max}(R) = \sup\{\rho s_1(1) \int_0^R x^{d-1} g_2^{yz}(x) dx\}, \tag{12}$$

where the notation $\sup\{\dots\}$ indicates the mathematical supremum. The function $Z_{max}(R)$ is thus a significantly more restrictive upper bound for candidate cross-correlation functions of a single solute sphere amongst same-size solvent spheres than for candidate pair correlation functions of packings of indistinguishable spheres.

The characteristics of DLP optimal packings in each dimension d are heavily dependent on the underlying differences in packing spheres densely in $\mathbb{R}^d$. For example, in $\mathbb{R}^2$ there is a unique arrangement of $K_2 = 6$ disks in contact with a central disk, whereas in $\mathbb{R}^3$ there are a continuum of arrangements of $K_3 = 12$ spheres in contact with a central sphere. In $\mathbb{R}^2$, there is a unique densest infinite packing of disks and in $\mathbb{R}^3$, there are an uncountably infinite number of densest infinite packings of spheres.

Differences in characteristics across dimension are also driven by the existence of particularly locally dense dimensionally-unique packings. In $\mathbb{R}^2$, these include the wedge hexagonal packings described in paper I and the curved hexagonal packings [7], the densest local packings for $N = 3k(k+1)$, $k = 1, 2, \dots 6$. In $\mathbb{R}^3$, they include the two perfectly icosahedrally symmetric packings for $N = 42$ and $N = 134$ (Table II) that contain only two and four shells, respectively. It is curious to note that both the curved hexagonal packings and the perfectly icosahedrally symmetric packings for $N = 42$ and $N = 134$ are composed of a relatively small number of densely-packed shells of spheres; however, in the curved hexagonal packings, the spheres in any given shell are in contact with one another whereas in the aforementioned perfectly icosahedrally symmetric packings, they are not.

Dimensions four, eight and twenty-four are similar to dimension two in that in each of these dimensions there is a unique (uniqueness is conjectured for $d = 4$ and proved for $d = 8$ and $d = 24$[2]) arrangement of spheres with kissing numbers $K_4 = 24$ (recently proved by Musin in [37]), $K_8 = 240$, and $K_{24} = 196560$. The densest known packings in dimensions four, eight, and twenty-four are also conjectured to be unique, and each is a lattice packing that is self-dual, i.e., its reciprocal lattice is itself (the dual of the triangular lattice is similarly a triangular lattice, though resized and rotated 30 degrees). The self-duality of

the E_8 ($d = 8$) and Leech ($d = 24$) lattices has been exploited to prove, up to a very small numerical tolerance, that identical nonoverlapping spheres with centers on the sites of these lattices are the densest packings of spheres in their respective dimensions [15]. In dimension five, the densest known packings can be described, similarly to Barlow packings, as stackings of layers of the densest packings in $\mathbb{R}^4$. Consequently, we might expect to find DLP optimal packings in $\mathbb{R}^d$, $d = 4$, 8, and 24 similar to the curved hexagonal packings in $\mathbb{R}^2$, whereas we would not expect to find such optimal packings in $\mathbb{R}^5$.

These and other dimension-dependent dense packing characteristics could have an effect on the probability of freezing in a overcompressed liquid of hard spheres in $\mathbb{R}^d$. Recent work [38–41] suggests that the phase transition from a overcompressed hard-sphere liquid in $\mathbb{R}^3$ to a crystalline solid with sphere centers near to the sites of the spheres centers in a Barlow packing may be described as a two-stage process. In the first stage, small clusters of spheres form that are denser than either the liquid or crystalline solid states. In the second stage, the dense clusters grow in size and decrease in density while their bulk (interior) transforms from the center outward into a crystalline solid state [40]. An analogy can be drawn between DLP optimal packings in $\mathbb{R}^3$ for smaller N and the small clusters, in that both are locally denser than corresponding subsets of Barlow packings or crystalline solid states and in that neither are similar (both angularly and radially) to small subsets of Barlow packings. A similar analogy applies between DLP optimal packings for sufficiently large N and the larger clusters with crystalline solid interiors, in that both are very similar to Barlow packings in their bulk and not similar on and near their surfaces.

In general, the probability per unit time of freezing in hard-sphere liquids at comparable overcompression decreases with increasing dimension, at least for dimensions two through six [42]. However, with the previously described two-stage process in mind, consideration of the dimension-dependent characteristics of the densest local packings could lead to a further increase, beyond what might otherwise be predicted by the general trend, in estimates of the probability per unit time of freezing in $\mathbb{R}^2$ as compared to in $\mathbb{R}^3$.

For example, unlike in $\mathbb{R}^3$, in $\mathbb{R}^2$ there are several values of $N > K_2 = 6$, specifically, $N = 12$, 30 and 54, for which one of the densest local packings is a subset of the densest infinite packing, and therefore for which the equality in the upper bound (2) can hold. We might expect to see this occurring in $\mathbb{R}^4$, $\mathbb{R}^8$, or $\mathbb{R}^{24}$ as well, but not in $\mathbb{R}^5$. The equivalence of densest local packings at certain N and subsets of the densest infinite packing in $\mathbb{R}^2$ suggests

that the first stage of the two-stage crystallization process, in which small clusters of spheres form that are denser than either the liquid or crystalline solid states, may be shortened in duration for hard-disk liquids in $\mathbb{R}^2$ relative to hard-sphere liquids in $\mathbb{R}^3$. If this is the case, accounting for the equivalence of densest local packings and subsets of the densest infinite packings should result in an increase in the probability per unit time of freezing in $\mathbb{R}^2$ and potentially $\mathbb{R}^4$, $\mathbb{R}^8$, and $\mathbb{R}^{24}$ as compared to in $\mathbb{R}^3$ and $\mathbb{R}^5$. For hard-sphere liquids at densities near the freezing point, in $\mathbb{R}^2$ relative to in $\mathbb{R}^3$, the more pronounced "shoulder" [43] appearing in pair correlation functions between the first and second nearest-neighbor distances could be evidence indicating such a shortened first stage.

This example and the similarities between DLP optimal packings and the nuclei described in the two-stage description of crystallization suggest that there may be an explicit connection between freezing in overcompressed hard-sphere liquids and DLP optimal packings. It would be interesting, in the context of a revised nucleation theory, to explore the relationship between nucleation and dense local clusters of spheres configured with centers near the sites of sphere centers in the densest local packings.

ACKNOWLEDGEMENTS:

S.T. thanks the Institute for Advanced Study for its hospitality during his stay there. This work was supported by the Division of Mathematical Sciences at the National Science Foundation under Award Number DMS-0804431 and by the MRSEC Program of the National Science Foundation under Award Number DMR-0820341.

Appendix A: Lower bounds on $R_{min}(N)$

Knowledge of the densest infinite packings in $\mathbb{R}^3$, the Barlow packings, allows $R_{min}(N)$ to be bounded both from above and below. A lower bound can be obtained through the observation that it is not possible to remove a finite number $N+1$ of spheres from an infinite Barlow packing and replace them by $N+1$ spheres packed as an optimal DLP packing. If this could be accomplished at even one value of N, then the Barlow packings would not be the only densest infinite packings of identical nonoverlapping spheres in $\mathbb{R}^3$, as this operation could be repeated *ad infinitum* to yield an infinite-volume packing fraction ϕ_*^∞ greater than or equal to $\pi/\sqrt{18}$.

Consider removing all $N+1$ spheres (including a central sphere) in a Barlow packing with centers within distance $R(N) = R_{min}(N) + \epsilon$ of the center of the central sphere, where $N = N'$ is chosen to include all spheres in the coordination shell at $R(N')$. We term the set of all such subsets of $N'+1$ spheres chosen from all Barlow packings $\mathbb{B}_{N'}$, similar to the $\mathbb{B}_N$ defined in Sec. III. Attempting to replace (without overlap) the removed spheres with a DLP packing of $N'+1$ spheres with optimal radius $R_{min}(N')$, we see that ϵ must be in the range $0 \leq \epsilon \leq 1$. If ϵ were less than 0, then the DLP packing wouldn't be optimal. If ϵ were greater than or equal to 1, then the Barlow packings would not be the only densest packings of identical nonoverlapping spheres in $\mathbb{R}^3$, as for $\epsilon \geq 1$, the DLP packing with optimal radius $R_{min}(N')$ can be always be placed such that none of its spheres overlaps any of the remaining spheres in the Barlow packing. This range of epsilon results in the lower bound $R_{min}(N') \geq R(N') - 1$, valid for any $R(N') \geq R_{min}(N')$ chosen as stated above.

In practice, ϵ may be reduced significantly below the value of 1. For example, as for certain N', $R(N') = R_{min}(N') + \epsilon$ varies between the packings in the set $\mathbb{B}_{N'}$, ϵ is reduced from unity by the difference between the largest and smallest $R(N')$ for these N'. More generally, the value of ϵ can be significantly reduced by investigating the geometric considerations of placing the $N+1$ spheres of any DLP optimal packing of radius $R_{min}(N)$ into the void created by removing N spheres from a Barlow packing. Reducing ϵ to a minimum possible value $\epsilon_{min}(N)$ results in the lower bound $R_{min}(N) \geq R(N) - \epsilon_{min}(N)$.

Appendix B: Barlow packings and similarity metric reference sets

Any set of $N+1$ spheres in a given $\mathbb{B}_N$ can be used as a reference set in the similarity metric (9). However, for $N > 0$, there are always multiple reference sets of $N+1$ spheres that will produce the same $\{\delta_i\}$ and consequently the same value of $\mathcal{S}$ for a given comparison set. For example, as the metric (9) is insensitive to the angular position of any sphere, for a furthest coordination shell that is not full, the same $\{\delta_i\}$ is produced regardless of which of the spheres in the furthest shell is included in the packing used as a reference set.

When these and all other degeneracies are taken into account, we find that for $\mathbb{B}_N$ including only packings of $s = 1, 3, 5, 7, 9, 11$, and 13 Barlow stacking layers, where all $\mathbb{B}_{1054}$ packings are constructed from 13 layers, there are $1, 1, 3, 6, 14, 31$ and 70 distinct sets $\{\delta_i\}$. For the N studied where the packings in $\mathbb{B}_N$ do not all have the same number of layers, the

packings in $\mathbb{B}_N$ include s, $s+1$, and sometimes $s+2$ layers. For these $\mathbb{B}_N$, the set of distinct $\{\delta_i\}$ is a subset of the set of distinct $\{\delta_i\}$ for any $\mathbb{B}_N$ including packings of only $s+2$ layers, and the number of distinct sets $\{\delta_i\}$ is between the number for $\mathbb{B}_N$ including only packings of s layers and for $\mathbb{B}_N$ including only packings of $s+2$ layers.

An intuitive analysis of the determination of the shells $\{\delta_i\}$ suggests that the presence of relatively fewer shells in a reference set can generally increase the value of $\mathcal{S}$. An increase of this sort does occur when shells are of radial width large enough such that the number of sphere centers within each shell approaches the number density of the packing, i.e., when radial width is on the order of a sphere's diameter. However, this is not the case for the $\{\delta_i\}$ derived from the sets in each $\mathbb{B}_N$. Indeed, direct analysis of the distribution of spheres within each individual shell δ_i confirms that spheres in DLP optimal packings for a given N are in general radially configured in a relatively small number of shells. That is, the radial positions of the sphere centers in DLP optimal packings are clustered around a smaller number of distances from the center of the central sphere, relative to the number of coordination shells in the packings in $\mathbb{B}_N$, and the large fraction of DLP optimal packings that are most similar to FCC-derived packings is not the result of a design-flaw in the similarity metric (9).

---

[1] A. B. Hopkins, F. H. Stillinger, and S. Torquato, J. Math. Phys. **51**, 043302 (2010).

[2] J. H. Conway and N. J. A. Sloane, *Sphere Packings, Lattices and Groups* (Springer, 1998).

[3] K. Schütte and B. L. van der Waerden, Math. Annalen **125**, 325 (1953).

[4] J. Leech, The Mathematical Gazette **40**, 22 (1956).

[5] K. Schütte and B. L. van der Waerden, Math Annalen **123**, 96 (1951).

[6] A. B. Hopkins, F. H. Stillinger, and S. Torquato, Phys. Rev. E **81**, 041305 (2010).

[7] B. D. Lubachevsky and R. L. Graham, Disc. Comp. Geom. **18**, 179 (1997).

[8] A. Lenard, Arch. Ration. Mech. Anal. **59**, 219 (1975).

[9] S. Torquato and F. Stillinger, J. Phys. Chem. B **106**, 8354 (2002).

[10] T. Kuna, J. L. Lebowitz, and E. R. Speer, J. Stat. Phys. **129**, 417 (2007).

[11] S. Torquato and F. H. Stillinger, Exp. Math. **15**, 307 (2006).

[12] A. B. Hopkins, F. H. Stillinger, and S. Torquato, Phys. Rev. E **79**, 031123 (2009).

[13] H. Cohn, A. Kumar, and S. Torquato, unpublished. The authors in this reference used the Z_{max}

realizability condition to improve upon the best known upper bounds [15] on the maximum infinite-volume packing fraction ϕ_*^∞ for identical nonoverlapping spheres in various dimensions, where the method employed by Cohn and Elkies in [15] relies only on particle pair information.

[14] T. C. Hales, Ann. Math. **162**, 1065 (2005).

[15] H. Cohn and N. Elkies, Ann. Math. **157**, 689 (2003).

[16] Supplementary materials can be found at <http://cherrypit.princeton.edu>.

[17] H. Pfoertner, *Densest packings of spheres in a sphere*, URL http://www.randomwalk.de/sphere/insphr/spheresinsphr.html.

[18] W. Barlow, Nature **29**, 186 (1883).

[19] H. Cohn and A. Kumar, Ann. Math. **170**, 1003 (2009).

[20] In practice, we find over the range of N studied in $\mathbb{R}^3$ that the only $N > 12$ for which $R_{min}(N) = R_{min}(N-1)$ is $N = 60$.

[21] R. M. L. Tammes, Rec. Trv. Bot. Neerl. **27**, 1 (1930).

[22] N. J. A. Sloane, R. H. Hardin, and W. D. Smith, *Tables of spherical codes*, URL www.research.att.com/~njas/packings/.

[23] For $N = 216$, $Z^S_{max}(R_{min}(216)) = 130$, and 130 is the last number for which optimal spherical codes are presented in [22].

[24] The Barlow packings consist of translated planes (layers) of contacting spheres with centers arranged on the sites of a triangular lattice, where the layers are "stacked" on top of one another. In the stackings, there are three possible translations relative to the central layer (the layer including the central sphere), denoted A, B, and C, obeying the rule that no layer can be consecutively repeated. We have found that it is only the positions of the A layers relative to the central layer that are relevant in determining the coordination shells about the central sphere. The FCC Barlow stacking, denoted by repeating ABC layers, is thus indistinguishable to the similarity metric from any other stacking with an A layer repeated every three layers.

[25] S. C. Mau and D. A. Huse, Phys. Rev. E **59**, 4396 (1999).

[26] M. R. Hoare and P. Pal, Adv. Phys. **20**, 161 (1971).

[27] J. A. Northby, J. Chem. Phys. **87**, 6166 (1987).

[28] J. P. K. Doye and D. J. Wales, Chem. Phys. Lett. **247**, 339 (1995).

[29] D. J. Wales and J. P. K. Doyes, J. Phys. Chem. A **101**, 5111 (1997).

[30] Y. Xiang, H. Jiang, W. Cai, and X. Shao, J. Phys. Chem. A **108**, 3586 (2004).

[31] D. J. Wales, J. P. K. Doye, A. Dullweber, M. P. Hodges, F. Y. Naumkin, F. Calvo, J. Hernandez-Rojas, and T. F. Middleton, *The cambridge cluster database*, URL `http://www-wales.ch.cam.ac.uk/CCD.html`.

[32] For $N = 42$, the V_{LJ} of the DLP and Lennard-Jones optimal configurations are -189.63125 and -202.36466 [31], respectively; for $N = 114$, the V_{LJ} are -634.02115 and -655.75631 [31], and for $N = 134$, the V_{LJ} are -733.11071 and -790.27812 [31].

[33] N. J. A. Sloane, R. H. Hardin, T. D. S. Duff, and J. H. Conway, Disc. Comp. Geom. **14**, 237 (1995).

[34] S. Torquato, T. M. Truskett, and P. G. Debenedetti, Phys. Rev. Lett. **84**, 2064 (2000).

[35] S. Torquato and F. H. Stillinger, J. Phys. Chem B **105**, 11849 (2001).

[36] In the diagrams of paper I, e.g., for DLP optimal packings in $\mathbb{R}^2$ for $N = 24$, $N = 45$ and $N = 95$ disks, it is difficult to perceive that the disks forming a cavity around the central disk are not all the same radial distance from the central disk. However, though the difference in radial distances between these disks is small, it is far larger than the precision to which the spatial positions of sphere centers are calculated by the algorithm.

[37] O. R. Musin, Ann. Math. **168**, 1 (2008).

[38] H. J. Schöpe, G. Bryant, and W. van Megen, Phys. Rev. Lett. **96**, 175701 (2006).

[39] H. J. Schöpe, G. Bryant, and W. van Megen, J. Chem. Phys. **127**, 084505 (2007).

[40] T. Schilling, H. J. Schöpe, M. Oettel, G. Opletal, and I. Snook, Phys. Rev. Lett. **105**, 025701 (2010).

[41] T. Kawasaki and H. Tanaka, Proc. Nat. Acad. Sci. **107**, 14036 (2010).

[42] J. A. van Meel, B. Charbonneau, A. Fortini, and P. Charbonneau, Phys. Rev. E **80**, 061110 (2009).

[43] T. M. Truskett, S. Torquato, S. Sastry, P. G. Debenedetti, and F. H. Stillinger, Phys. Rev. E **58**, 3083 (1998).